https://doi.org/10.5194/egusphere-2026-2589
Preprint. Discussion started: 20 May 2026

Snow Structure Modulates the Isotopic Imprint of Sublimation

Shaakir Dar[1,2], Olga Silantyeva[2], Pertti Ala-aho[1], Benjamin Walter[3], John Hult[2], Valtteri Hyöky[1], Jeffrey Welker[4,5], Hannu Marttila[1]

[1] Water, Energy and Environmental Engineering Research Unit, University of Oulu, Oulu 90570, Finland
[2] Department of Geosciences, University of Oslo, Oslo 0371, Norway
[3] WSL Institute for Snow and Avalanche Research, Davos 7260, Switzerland
[4] Department of Biological Sciences, University of Alaska Anchorage, AK 99508 United States of America.
[5]Ecology and Genetics Research Unit, University of Oulu, Oulu 90570, Finland.

Correspondence to: Shaakir Dar (shaakir.dar@oulu.fi)

Abstract. Sublimation modifies the stable isotopic composition of snow. The physical controls governing this imprint, particularly the interplay between isotopic fractionation, snow structure, and airflow, remain poorly constrained. Current surface-exchange models commonly treat sublimation fractionation as a function of atmospheric forcing and boundary-layer exchange, with limited explicit representation of snow structural state. Here, we present controlled wind-tunnel experiments examining sublimation-driven isotopic changes ($\delta^{18}O$, $\delta^{2}H$, and d-excess) in three contrasting snow types (laboratory snow, fresh natural snow, and old natural snow) under varied airflow regimes, ambient humidity, and basal-to-air temperature contrasts. We show that airflow is the dominant experimental control on sublimation mass loss, but bulk isotopic change does not scale directly with mass loss, revealing a partial decoupling between sublimation magnitude and isotopic modification. High airflow produced the smallest isotopic change per unit mass loss, consistent with strong turbulent exchange reducing the isotopic imprint of sublimation. However, absolute isotopic change varied systematically with snow structural state, scaling strongly with bulk porosity in natural snow. This structural dependence weakened after mass normalization for $\delta^{18}O$ and $\delta^{2}H$, but persisted for d-excess, suggesting that properties associated with porosity influence effective kinetic fractionation in addition to cumulative isotopic change. Laboratory snow deviated from this behavior: despite overlapping the porosity range of natural snow, it showed no porosity-isotopic change relationship. This suggests that bulk porosity alone is insufficient to capture the structural controls on isotopic response to sublimation. Within a relative snow-type comparison, the Craig–Gordon model systematically overpredicted $\delta^{18}O$ and $\delta^{2}H$ enrichment and underpredicted the range of d-excess change. The systematic nature of these discrepancies suggests that parameter uncertainty alone is unlikely to explain the mismatch and points to missing representation of internal vapor transport through the snow pore network. Our study shows that sublimation rate alone is insufficient to predict isotopic modification; snow structural state must be considered alongside atmospheric forcing in models of sublimation-driven isotopic evolution. Snow structural state can therefore impose a systematic overprint on isotopic signals in snow archives and meltwater that structure-independent models are likely to misrepresent.

https://doi.org/10.5194/egusphere-2026-2589
Preprint. Discussion started: 20 May 2026

1 Introduction

Seasonal snow is a major freshwater reservoir for nearly two billion people, and ongoing warming is rapidly altering snow accumulation, persistence, and the timing and magnitude of freshwater release (Gottlieb and Mankin, 2024; Mankin et al., 2015; Mote et al., 2018). Sublimation can remove 10-90% of snowfall in cold regions (Gascoin, 2021; Reba et al., 2012; Sexstone et al., 2018; Stigter et al., 2018; Strasser et al., 2008). As atmospheric evaporative demand intensifies under climate change (Allan et al., 2023), sublimation is expected to rise further and exert an increasingly important role in snow mass balance, surface energy exchange, and landscape water balances.

Beyond water loss, sublimation also modifies the stable isotopic composition of snow (Beria et al., 2018; Dansgaard, 1964), typically expressed in terms of oxygen-18 ($\delta^{18}O$), deuterium ($\delta^{2}H$), and deuterium excess (d-excess = $\delta^{2}H - 8 \cdot \delta^{18}O$). Snow, firn, and ice isotopes underpin interpretations of moisture source, atmospheric circulation, and paleoclimate variability (Casado et al., 2020, 2021; Klein et al., 2016; MacGregor et al., 2020; Munroe and Spötl, 2026; Wahl et al., 2022) and are widely used in catchment isotope hydrology to trace storage and release pathways (Ala-aho et al., 2017; Laudon et al., 2004; Sprenger et al., 2022). However, post-depositional exchange and phase changes during dry and wet snow metamorphism can overprint precipitation signals after deposition, complicating both ice-core interpretation and isotope-based water-balance inferences (Earman et al., 2006; Noor et al., 2023b, a; Wahl et al., 2022). Sublimation enriches residual snow in heavy isotopes and reduces d-excess, consistent with kinetic fractionation under non-equilibrium conditions. Yet the magnitude of this isotopic change varies in ways that mass loss alone cannot explain (Harris Stuart et al., 2023; Wahl et al., 2024). Materials at comparable sublimation rates can exhibit very different isotopic responses depending on internal structure and vapor transport pathways, with porous snow exhibiting substantially stronger responses than low-porosity ice (Bellagamba et al., 2024; Sokratov and Golubev, 2009).

This variability arises because sublimation in snow is fundamentally a porous-medium problem. Unlike evaporation from an open water surface, sublimation in snow operates within a three-dimensional porous matrix where vapor transport, phase change, and isotopic fractionation occur simultaneously at multiple spatial scales, from individual grain surfaces to the full snowpack depth. Isotopic modification reflects the coupled action of boundary-layer exchange with the atmosphere, vapor diffusion and advection within the pore space, and internal phase changes driven by temperature gradients and evolving snow microstructure (Calonne et al., 2014; Ebner et al., 2016; Fourteau et al., 2021; Harris Stuart et al., 2023; Jafari et al., 2020, 2022; Johnsen et al., 2000; Neumann and Waddington, 2004). In natural snowpacks, temperature gradients between the snow surface and the ground sustain internal vapor fluxes through temperature gradient metamorphism (TGM), the sublimation of ice at warmer grain faces and condensation at cooler ones (Colbeck, 1983; Sturm and Benson, 1997). These fluxes are themselves isotopically fractionating and progressively modify snow microstructure by promoting grain growth and increasing pore connectivity (Ebner et al., 2016, 2017; Johnsen et al., 2000). At the same time, wind alters boundary-

https://doi.org/10.5194/egusphere-2026-2589
Preprint. Discussion started: 20 May 2026

layer resistance and drives pore-space ventilation, further influencing vapor transport and residence time (Albert, 2002; Neumann and Waddington, 2004). These processes operate simultaneously, linking atmospheric forcing, internal vapor dynamics, and evolving snow structure, making them difficult to isolate using field observations alone.

Existing modelling frameworks reflect a similar surface-process limitation. The Craig-Gordon framework (Craig and Gordon, 1965), originally developed for evaporation from open-water surfaces, parameterizes fractionation as a single-stage interfacial process governed by equilibrium fractionation and boundary-layer resistance. Numerous studies have extended this framework to snow and firn by incorporating multilayer representations or parameterized internal vapor exchange (Casado et al., 2020; Madsen et al., 2019; Neumann and Waddington, 2004; Wahl et al., 2022), representing important advances. Nevertheless, internal vapor transport is typically represented through bulk or steady-state parameters rather than being explicitly linked to measurable snow physical properties such as porosity or pore connectivity. The conditions under which this mismatch becomes consequential remain poorly constrained.

While many studies have documented sublimation-driven isotopic enrichment in snow and firn (Earman et al., 2006; Hughes et al., 2021; Sokratov and Golubev, 2009; Wahl et al., 2022), the physical controls determining the magnitude of isotopic modification across snow structural states and airflow regimes remain poorly quantified under controlled conditions. Existing laboratory studies have either used isothermal setups that suppress temperature-gradient metamorphism, focused on a single snow type, or varied atmospheric forcing without isolating the structural controls on isotopic response. To our knowledge no controlled experiment has simultaneously examined the roles of airflow regimes, snow structural state (spanning natural types and laboratory-produced snow) and thermal gradient forcing on sublimation-driven isotopic evolution, nor systematically evaluated Craig-Gordon model performance across these conditions. Here, we address this gap with controlled wind-tunnel experiments that combine sublimation with non-isothermal snow conditions while spanning contrasting snow types, airflow regimes, air temperatures, and relative humidities. We aim to: (i) quantify sublimation mass loss and associated isotopic changes across atmospheric forcing conditions and snow types; (ii) establish how isotopic response scales with snow structural state and airflow regime relative to sublimation magnitude; and (iii) evaluate Craig–Gordon surface-fractionation predictions across this parameter space and identify the structural and atmospheric conditions under which surface-only formulations diverge from observations.

2. Methods

2.1 Experimental Facility

The sublimation experiments were conducted in the Cold Climate Container (C3) at the Department of Geosciences, University of Oslo, Norway. The C3 is an advanced environmental simulation facility composed of two integrated systems: a snow production module and a wind tunnel (Figure 1). The two systems share a common temperature-controlled aluminium

https://doi.org/10.5194/egusphere-2026-2589
Preprint. Discussion started: 20 May 2026

base plate that can be slid on rails and translated between the snow production module and the wind tunnel. The wind tunnel itself is mounted on a vertical lift and is lowered onto the base plate, sealing against rubber gaskets to form an enclosed flow channel. The air temperature inside the container can be regulated between −40 and +20 °C, allowing stable and reproducible experimental conditions.

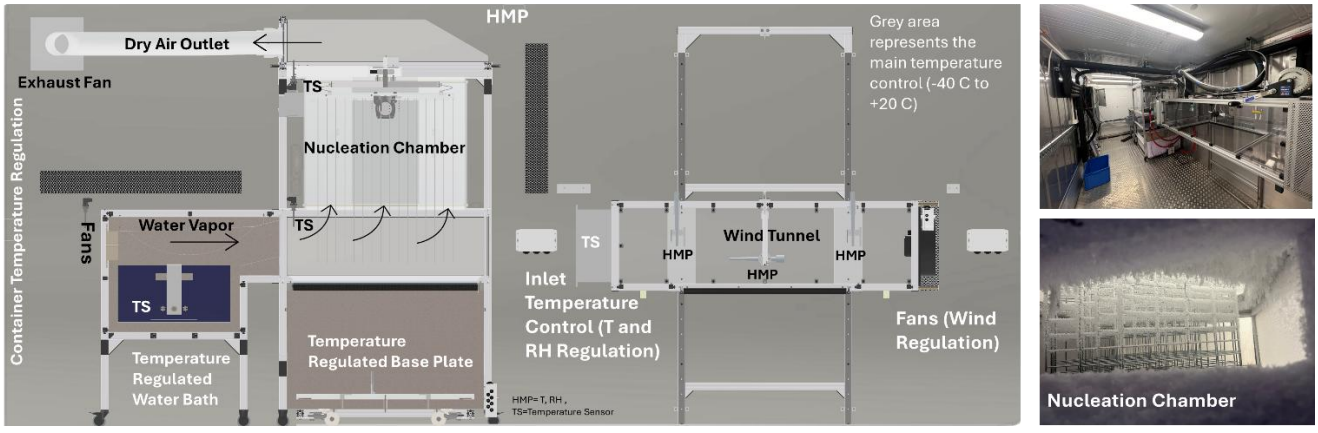

Figure 1. Schematic layout and photographs of the Cold Climate Container (C3) facility at the University of Oslo used for the sublimation experiments. The left panel shows a plan-view schematic of the container, highlighting the snow production module (temperature-regulated water bath, vapor flow fans, and nucleation chamber) and the wind tunnel system. Grey shaded areas indicate the main container temperature control range (−40 to +20 °C). The inlet temperature control unit allows independent regulation of air temperature and relative humidity entering the wind tunnel. Airflow through the tunnel is generated by adjustable outlet fans located at the downstream end of the tunnel. Locations of temperature sensors (TS) and humidity-temperature probes (HMP155) are indicated. The right panels show photographs of the wind tunnel installed inside the container (top) and the nucleation chamber during snow production (bottom).

The snow production module is a modified version of the Snow Maker described by Schleef et al. (2014). It consists of a temperature-controlled water bath, a set of fans that direct water vapor, and a nucleation chamber where vapor deposits as ice crystals onto a nucleation net. The net is periodically vibrated to release the accumulated snow crystals, which are collected on a temperature-regulated aluminium base plate.

The wind tunnel has a rectangular cross-section (H = 40 cm, W = 80 cm, L = 140 cm) with transparent plexiglass walls and is mounted on a vertical lift mechanism that allows it to be raised and lowered onto the base plate to seal the flow channel. Airflow is generated by two adjustable outlet fans (Systemair AW Sileo 300 EC), which draw air through the tunnel from an upstream inlet. Fan rotation can be controlled to produce maximum airflow velocities of up to ~3 m s^{-1}. Airflow velocity is used as a relative airflow proxy rather than a direct measure of boundary-layer thickness or near-surface shear stress. Airflow velocity at the snow surface was not measured directly; instead, fan rotational speed (rpm) was varied to impose different airflow regimes and is used here to distinguish relative airflow intensity among experiments. Therefore, interpretations of boundary-layer processes are qualitative and based on relative airflow differences rather than direct measurements of near-surface flow.

https://doi.org/10.5194/egusphere-2026-2589
Preprint. Discussion started: 20 May 2026

The temperatures of the base plate and the wind tunnel inlet airflow were independently regulated between −20 and +20 °C using separate ultra-low refrigerated/heating circulators (JULABO FP51-SL; temperature stability ±0.05 °C). Inlet air temperature was controlled using a duct-mounted water heating coil (Systemair VBR 80-40-2) integrated at the wind tunnel inlet. Relative humidity within the wind tunnel was regulated by adjusting the temperature difference between the container air and the inlet airflow. The wind tunnel was instrumented with three Vaisala HMP155 sensors positioned at the inlet, midpoint, and outlet of the airflow channel, measuring air temperature, relative humidity, frost/dew point temperature, and water vapor mixing ratio.

2.2 Snow Types and Petri Dish Setup

Three snow types were prepared, spanning a range of bulk porosity and microstructural states: (1) laboratory-produced snow (LS), generated within the C3 facility (Section 2.1) following the method of Schleef et al. (2014), consisting of columnar and plate-like crystals; (2) freshly fallen natural snow (FS), collected outdoors and immediately cold-stored at −18°C to preserve initial microstructure, consisting of dendritic crystals; and (3) old natural snow (OS), excavated from the lower seasonal snowpack and consisting of small rounded grains, representing aged, partially metamorphosed snow. Mean bulk densities (n = 8 per type) were 0.23 ± 0.04 g cm^{-3} for FS, 0.28 ± 0.02 g cm^{-3} for LS, and 0.31 ± 0.02 g cm^{-3} for OS, corresponding to mean porosities of 0.75, 0.70, and 0.66, respectively.

For each snow type, the material was gently placed into Petri dishes (14 cm diameter, 2 cm height; empty dish mass = 49.66 g). Snow surfaces were carefully levelled to produce a uniform, planar surface and to minimize variability in exposed surface area. Bulk density (ρ_{bulk}) and porosity (φ) were calculated as

$$\rho_{bulk} = \frac{m_0}{V} \quad (1)$$

$$\varphi = 1 - \frac{\rho_{bulk}}{\rho_i} \quad (2)$$

,

where m_0 is the initial snow mass and V is the dish volume and ice density $\rho_i = 917\ \mathrm{kg\ m^{-3}}$. Bulk porosity is used as an experimentally accessible first-order proxy for snow structural properties relevant to vapor exchange, including pore connectivity, permeability, and specific surface area available for vapor exchange (Calonne et al., 2012), while acknowledging that metamorphic history introduces structural differences beyond bulk porosity alone (Pinzer et al., 2012; Schneebeli and Sokratov, 2004). Because pore connectivity, tortuosity, permeability, specific surface area, and surface

https://doi.org/10.5194/egusphere-2026-2589
Preprint. Discussion started: 20 May 2026

roughness were not measured directly, porosity is treated here as an empirical structural proxy rather than as a unique mechanistic variable.

Each experiment lasted 24 hours. At the end of each experiment, Petri dishes were weighed using a high-precision analytical balance (Sartorius GmbH, Type B310S; corner-load tolerance ±0.004 g), and sublimation mass loss was determined from the difference between initial and final snow mass. Prior to loading the snow into Petri dishes, representative subsamples of each snow type were collected for initial isotopic composition analysis. Final isotope samples were collected as bulk samples integrating the full remaining snow depth in each Petri dish. Samples were melted and homogenized prior to analysis, so the reported final isotope values represent depth-integrated bulk compositions

The experimental configuration resulted in the following thermal boundary conditions within the snow samples. The base plate was maintained at −1°C for all experiments, while the surrounding airflow was maintained at subfreezing temperatures (see Section 2.3). Snow samples were held in polypropylene Petri dishes (thermal conductivity ~0.15-0.20 W m^{-1} K^{-1}; base thickness ~1.5 mm), which provided partial thermal insulation between the base plate and the snow, while the dish sides were exposed to the surrounding airflow. As a result, the thermal field within the snow was three-dimensional (Dick et al., 2026): the base was moderately warmed through conduction from the base plate, whereas the sides and upper surface were controlled by the surrounding airflow. Consequently, effective vertical temperature gradients across the ~2 cm snow depth were substantially smaller than would be expected from the difference between base plate and air temperatures alone. This configuration maintains a non-isothermal snowpack and supports coupled surface sublimation and temperature-gradient metamorphism.

2.3 Environmental Conditions Across Experiments

Figure 2 summarizes the thermal and hygrometric conditions maintained during the experimental runs. Across EXP1-EXP8, mean air temperatures within the wind tunnel ranged from approximately −22 to −2 °C, while mean relative humidity ranged from approximately 25% to 85%. The base plate was maintained at a constant −1 °C for all experiments.

Air temperature and relative humidity were generally uniform along the wind tunnel within each experiment. Differences among inlet, midpoint, and outlet sensors were typically within ~2 °C for temperature and ~10% RH for relative humidity, indicating limited spatial variability in atmospheric conditions.

Airflow intensity was controlled using fan rotational speed (rpm), producing three distinct regimes: (i) zero-airflow, fan-off condition (0 rpm; EXP5 and EXP8), corresponding to a bulk airflow velocity of 0 m s^{-1}, (ii) low airflow (~256-258 rpm; EXP1-EXP3), with a bulk velocity of ~0.7 m s^{-1}, and (iii) high airflow (~1930-1970 rpm; EXP4, EXP6, and EXP7), corresponding to ~3 m s^{-1}. These velocities represent bulk tunnel flow rather than near-surface wind speed at the snow

https://doi.org/10.5194/egusphere-2026-2589
Preprint. Discussion started: 20 May 2026

surface and span conditions from diffusion-dominated transport to strongly forced airflow, allowing controlled investigation of sublimation and isotopic evolution across a range of transport regimes.

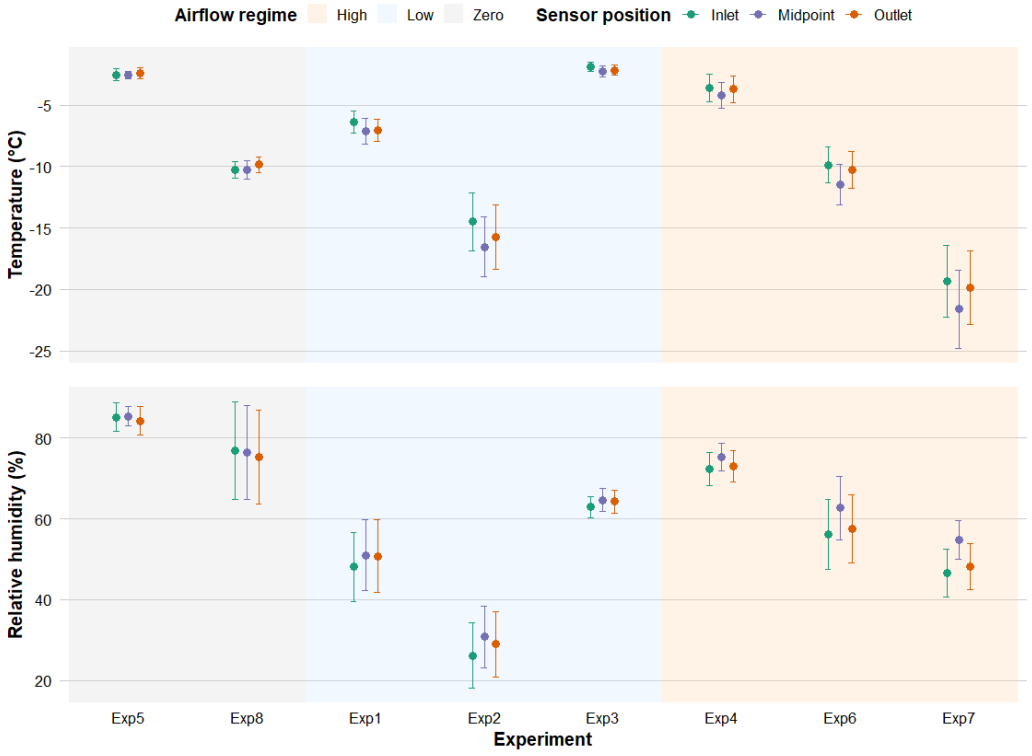

Figure 2. Air temperature (top) and relative humidity (bottom) measured along the wind tunnel at inlet, midpoint, and outlet positions for experiments EXP1-EXP8. Experiments are ordered and grouped by airflow regime, with shaded regions indicating zero flow (grey), low airflow (blue), and high airflow (peach).

2.4 Isotopic Analysis

Snow samples were collected in double-sealed polyethylene bags, thawed at room temperature, transferred to 15 mL vials, and stored at 4°C until analysis. All analyses were completed within one month. Stable water isotope ratios ($\delta^{18}O$ and $\delta^{2}H$) were measured at the University of Oulu Geolab using cavity ring-down spectroscopy with a Picarro L2140-i analyser. Instrumental accuracy was ±0.025‰ for $\delta^{18}O$ and ±0.1‰ for $\delta^{2}H$. Results were normalized to VSMOW2 (Vienna Standard Mean Ocean Water) using two reference standards: VIRO ($\delta^{18}O = -11.2$‰, $\delta^{2}H = -84.5$‰) and TAP ($\delta^{18}O = -21.0$‰, $\delta^{2}H = -156$‰). Each sample was injected seven times; the first three were discarded and the mean of the remaining four reported (Penna et al., 2012; Qu et al., 2019).

Two complementary metrics were used to quantify isotopic enrichment relative to mass loss. The mass-normalized isotopic change (IC, ‰ g^{-1}) is defined as

https://doi.org/10.5194/egusphere-2026-2589
Preprint. Discussion started: 20 May 2026

$$IC = \frac{\Delta(\delta)}{\Delta m} \quad (3)$$

where Δ(δ) represents the change in $\delta^{18}O$, $\delta^{2}H$, or d-excess, and Δm is the sublimated mass.

The fraction-normalized isotopic change (IC*, ‰ per unit fractional mass loss) is defined as

$$IC^{*} = \frac{\Delta(\delta)}{\Delta m / m_0} \quad (4)$$

where $m_0$is the initial sample mass. Because IC and IC* are ratios, their uncertainty increases when mass loss is small. Normalized values from zero-airflow experiments are therefore interpreted with greater caution than absolute isotope changes.

2.5 Craig-Gordon Modelling: Static and Time-Stepping Finite-Reservoir Formulations

Sublimation-driven isotopic changes in snow were simulated using the Craig-Gordon (CG) (Craig and Gordon, 1965) model to estimate the isotopic composition of vapor flux leaving the snow surface. This vapor flux was subsequently coupled to a finite-reservoir isotope mass balance to predict the evolution of bulk snow isotopic composition during sublimation. For each experiment, the snow surface was treated as the sublimating reservoir with isotopic composition equal to the initial bulk value δ_0. In δ-notation, the Craig-Gordon expression for the sublimating vapor is

$$\delta_E = \frac{\delta_s - \varepsilon^{*} - RH(\delta_a + \varepsilon_k)}{1 - RH + \varepsilon_k/1000} \quad (5)$$

where δ_E, δ_s, and δ_a are the isotopic compositions of the sublimating vapor, the snow surface, and the ambient vapor, respectively; In all Craig–Gordon calculations, RH is expressed as a fraction from 0 to 1 and normalized with respect to ice at the relevant temperature; ε* is the equilibrium fractionation factor (‰); and ε_k is the kinetic fractionation factor (‰). Equilibrium fractionation factors were calculated using the temperature-dependent ice-vapor relationships of Ellehoj et al., (2013). Kinetic fractionation was parameterized following the aerodynamic resistance formulation of (Gat, 1996),

$$\varepsilon_k = (1 - RH)\, n\, c_D \times 10^3 \quad (6)$$

where n is the airflow-regime resistance factor (n was set to 1 for zero-airflow, 0.7 for low airflow, and 0.5 for high-airflow in the experiments) and c_D is the diffusivity contrast $c_D = (D_M / D_i) - 1$. with D_M and D_i the molecular diffusivities of the light and heavy isotopologues, respectively. Using diffusivities from (Merlivat, 1978) : $D_M/D_i = 1.0251$ for $\delta^{2}H$ and $D_M/D_i = 1.0285$ for $\delta^{18}O$.

2.5.1 Static Craig-Gordon Finite-Reservoir Isotope Mass Balance

Assuming each snow sample behaves as a finite, well-mixed reservoir, isotopic mass balance during sublimation is expressed here in δ-notation using a linear approximation. While exact mass balance is defined in ratio space, this

https://doi.org/10.5194/egusphere-2026-2589
Preprint. Discussion started: 20 May 2026

formulation is appropriate for the small (‰-scale) isotopic changes observed in these experiments. Conservation of heavy isotopes can therefore be written as:

$$M_0\delta_0 = M_f\delta_f + M_{\text{loss}}\delta_E \tag{7}$$

where M_0 and δ_0 are the initial snow mass and isotopic composition, M_f and δ_f are the final mass and isotopic composition, and $M_{\text{loss}} = M_0 - M_f$ is the sublimated mass.

Solving for the final isotopic composition yields

$$\delta_f = \frac{M_0\delta_0 - M_{\text{loss}}\delta_E}{M_f} \tag{8}$$

Expressed in terms of the remaining mass fraction $f = M_f/M_0$, this simplifies to

$$\delta_f = \frac{\delta_0 - (1-f)\delta_E}{f} \tag{9}$$

This static formulation was applied independently to $\delta^{18}O$ and δ^2H, after which d-excess was computed as

$$d - excess = \delta^2H - 8\times\delta^{18}O \tag{10}$$

2.5.2 Time-Stepping Craig-Gordon Model with Evolving Snow Composition

The static formulation assumes that the isotopic composition of the sublimating surface (δ_s) remains fixed at its initial value δ_0. To account for progressive enrichment of the snow reservoir during sublimation, a time-stepping version of the CG model was implemented.

Each experiment is characterized by an initial mass M_0, final mass M_f, and total mass loss $M_{\text{loss}} = M_0 - M_f$. Sublimation was discretized into N equal mass increments,

$$\Delta M = \frac{M_{\text{loss}}}{N} \tag{11}$$

At time step k, the snow reservoir has mass M_k and isotopic composition $\delta_{s,k}$, with initial conditions

$$M_0 = M_0^{\text{obs}}, \delta_{s,0} = \delta_0^{\text{obs}} \tag{12}$$

The isotopic composition of vapor removed at step k is computed as

$$\delta_{E,k} = \frac{\delta_{s,k} - \varepsilon^* - RH(\delta_a + \varepsilon_k)}{1 - RH + \varepsilon_k/1000} \tag{13}$$

Finite-reservoir mass balance then gives

$$M_{k+1} = M_k - \Delta M \tag{14}$$

$$\delta_{s,k+1} = \frac{M_k\delta_{s,k} - \Delta M\delta_{E,k}}{M_{k+1}} \tag{15}$$

After N steps, the modelled final snow isotopic composition is

$$\delta_{f,\text{CG,ts}} = \delta_{s,k} \tag{16}$$

https://doi.org/10.5194/egusphere-2026-2589
Preprint. Discussion started: 20 May 2026

with d-excess computed as

$$d_{\mathrm{CG,ts}} = \delta^2\mathrm{H}_{f,\mathrm{CG,ts}} - 8\,\delta^{18}\mathrm{O}_{f,\mathrm{CG,ts}} \quad (17)$$

Sublimation was discretized into N=1440 equal mass-loss increments, with the snow isotopic composition updated after each increment. Sensitivity tests confirmed convergence: predictions were stable well within instrumental precision (±0.025‰ for $\delta^{18}O$, ±0.1‰ for δ^2H) for $N \geq 200$. Compared to a higher-resolution reference solution at N=5000, the N=1440 predictions deviated by at most 0.004‰ in $\delta^{18}O$ and 0.031‰ in δ^2H, well below instrumental precision. The mass-stepping scheme provides a numerically stable approximation of continuous sublimation-driven enrichment and does not represent a physical time discretization.

2.5.3 Relative Isotopic Change Comparison

Because the isotopic composition of ambient vapor (δ_a) was not directly measured during the wind-tunnel experiments, a reference-based relative enrichment framework was used to analytically eliminate δ_a from both static and time-stepping CG predictions. This cancellation assumes that ambient vapor isotopic composition is common to all snow types within a given experiment.

Let snow type i be the reference case and snow type j a comparison case. Observed isotopic changes are defined as

$$\Delta\delta_{\mathrm{obs},j} = \delta_{f,j} - \delta_{0,j}, \Delta\delta_{\mathrm{obs},i} = \delta_{f,i} - \delta_{0,i} \quad (18)$$

and the observed relative enrichment is

$$\Delta\delta_{\mathrm{rel,obs},j} = \Delta\delta_{\mathrm{obs},j} - \Delta\delta_{\mathrm{obs},i} \quad (19)$$

For the static CG formulation,

$$\Delta\delta_{\mathrm{rel,CG},j} = \left(\delta_{f,\mathrm{CG},j} - \delta_{0,j}\right) - \left(\delta_{f,\mathrm{CG},i} - \delta_{0,i}\right) \quad (20)$$

and the residual enrichment is

$$\Delta\varepsilon_{\mathrm{tot},j} = \Delta\delta_{\mathrm{rel,obs},j} - \Delta\delta_{\mathrm{rel,CG},j} \quad (21)$$

For the time-stepping CG formulation,

$$\Delta\delta_{\mathrm{rel,CG,ts},j} = \left(\delta_{f,\mathrm{CG,ts},j} - \delta_{0,j}\right) - \left(\delta_{f,\mathrm{CG,ts},i} - \delta_{0,i}\right) \quad (22)$$

$$\Delta\varepsilon_{\mathrm{tot,ts},j} = \Delta\delta_{\mathrm{rel,obs},j} - \Delta\delta_{\mathrm{rel,CG,ts},j} \quad (23)$$

Because δ_a cancels analytically in this relative framework, both $\Delta\varepsilon_{\mathrm{tot}}$and $\Delta\varepsilon_{\mathrm{tot,\,ts}}$quantify snow-type-specific deviations from CG predictions. Differences between the two metrics isolate the extent to which progressive isotopic change of the residual snow during sublimation influences model–data agreement.

2.5.4 Sensitivity analysis

o test whether CG-predicted snow-type contrasts were mainly caused by differences in initial isotope composition or by differences in remaining mass fraction, we performed a sensitivity analysis within the relative-change framework. For each

https://doi.org/10.5194/egusphere-2026-2589
Preprint. Discussion started: 20 May 2026

snow type pair and each experiment, four CG time-stepping simulations were run: i) each snow type uses its own δ^0 and f, giving the actual CG prediction; (ii) the non-reference snow type uses its own δ^0 but the reference f, isolating the δ^0 contribution; (iii) the non-reference snow type uses the reference δ^0 but its own f, isolating the f contribution; and (iv) both use the reference δ^0 and f, the zero baseline by definition. Relative isotopic change for each scenario was computed as
300 defined in Section 2.5.3, and the percentage contributions of δ^0 and f to the total CG prediction were calculated as $rel_B/rel_A \times 100$ and $rel_C/rel_A \times 100$, respectively. Because the CG model is nonlinear, these contributions are not strictly additive; an interaction term ($rel_A - rel_B - rel_C$) was computed to quantify the degree of coupling between δ^0 and f. The analysis was repeated for all three reference snow type choices (LS, FS, OS).

3. Results

305 ### 3.1 Sublimation Mass Loss and Isotopic Evolution of Snow Types Under Varying Airflow Conditions

Figure 3 summarizes the gravimetric and isotopic evolution of the three snow types across the eight experiments. While mass loss varied most clearly with airflow regime and remained similar across snow types within a given experiment, isotopic changes vary strongly with snow type. The three snow types span a range of initial physical properties, with fresh snow (FS) characterized by higher porosity (0.71–0.81) and lower density (0.18–0.26 g cm^{-3}), laboratory snow (LS) by
310 intermediate porosity (0.66–0.72) and higher density (0.25–0.31 g cm^{-3}), and aged snow (OS) exhibiting the lowest porosity (0.64–0.71) and highest densities (0.27–0.33 g cm^{-3}).

Absolute snow mass losses ranged from 2.4 to 20.9 g, corresponding to 2.4–25.6% of initial mass. Under zero-airflow conditions, EXP5 produced 2.4–2.7 g (2.4–3.4%) and EXP8 yielded 5.0–5.5 g (5.2–6.2%), with snow types differing by no
315 more than 1 percentage point within each experiment. Low-airflow experiments generated intermediate losses of 5.7–10.4 g (5.5–17.7%), while high-airflow conditions produced the largest losses, reaching 20.3–20.9 g (24.7–25.6%) in EXP6 and 16.5–17.9 g (17.7–24.4%) in EXP4. Across all airflow regimes, the three snow types consistently lost comparable mass fractions, indicating that the airflow regime imposed was the dominant across-experiment control on sublimation magnitude.

In contrast, isotopic responses diverged strongly among snow types and airflow conditions (Figures 3d-f). In all experiments,
320 sublimation enriched the residual snow in heavy isotopes ($\delta^{18}O$ and δ^2H) and reduced d-excess, consistent with kinetic fractionation under non-equilibrium conditions. However, the magnitude of isotopic change was not proportional to mass loss. Across all experiments, fresh snow (FS) consistently exhibited the strongest enrichment in $\delta^{18}O$ and δ^2H within every experiment, while laboratory snow (LS) showed the weakest response and aged snow (OS) intermediate but variable behaviour, with no consistent ordering between OS and LS.

325 The largest isotopic enrichments occurred under low-airflow conditions, despite only moderate mass losses. For example, in EXP2, FS enriched by +3.14 ‰ in $\delta^{18}O$ and +13.0 ‰ in δ^2H, with a −12.2 ‰ decline in d-excess, whereas LS, despite losing

https://doi.org/10.5194/egusphere-2026-2589
Preprint. Discussion started: 20 May 2026

a comparable mass fraction, enriched by only +1.48 ‰ and +7.10 ‰, respectively. Under zero-airflow conditions, limited sublimation also produced measurable isotopic changes. In EXP5, FS lost only 2.6 g (3.4%) yet enriched by +1.10 ‰ in $\delta^{18}O$ and +6.34 ‰ in $\delta^{2}H$, with a −2.49 ‰ change in d-excess. These results demonstrate that isotopic fractionation can be substantial even when total mass loss is small.

Under high-airflow conditions, isotopic enrichment was consistently reduced despite much larger mass losses. In EXP6, all snow types lost approximately 25% of their mass, yet $\delta^{18}O$ enrichment ranged only from +0.98 to +1.56 ‰ and $\delta^{2}H$ from +2.68 to +7.37 ‰. While FS remained the most enriched for $\delta^{18}O$ and $\delta^{2}H$, differences among snow types were smaller than under low airflow. In contrast to $\delta^{18}O$ and $\delta^{2}H$, patterns in d-excess were more variable across airflow regimes. Under low airflow, FS most frequently exhibited the largest decreases in d-excess, whereas under high airflow this ordering broke down, with FS, OS, and LS each showing the strongest response in different experiments. Zero-airflow conditions also showed mixed behaviour.

https://doi.org/10.5194/egusphere-2026-2589
Preprint. Discussion started: 20 May 2026

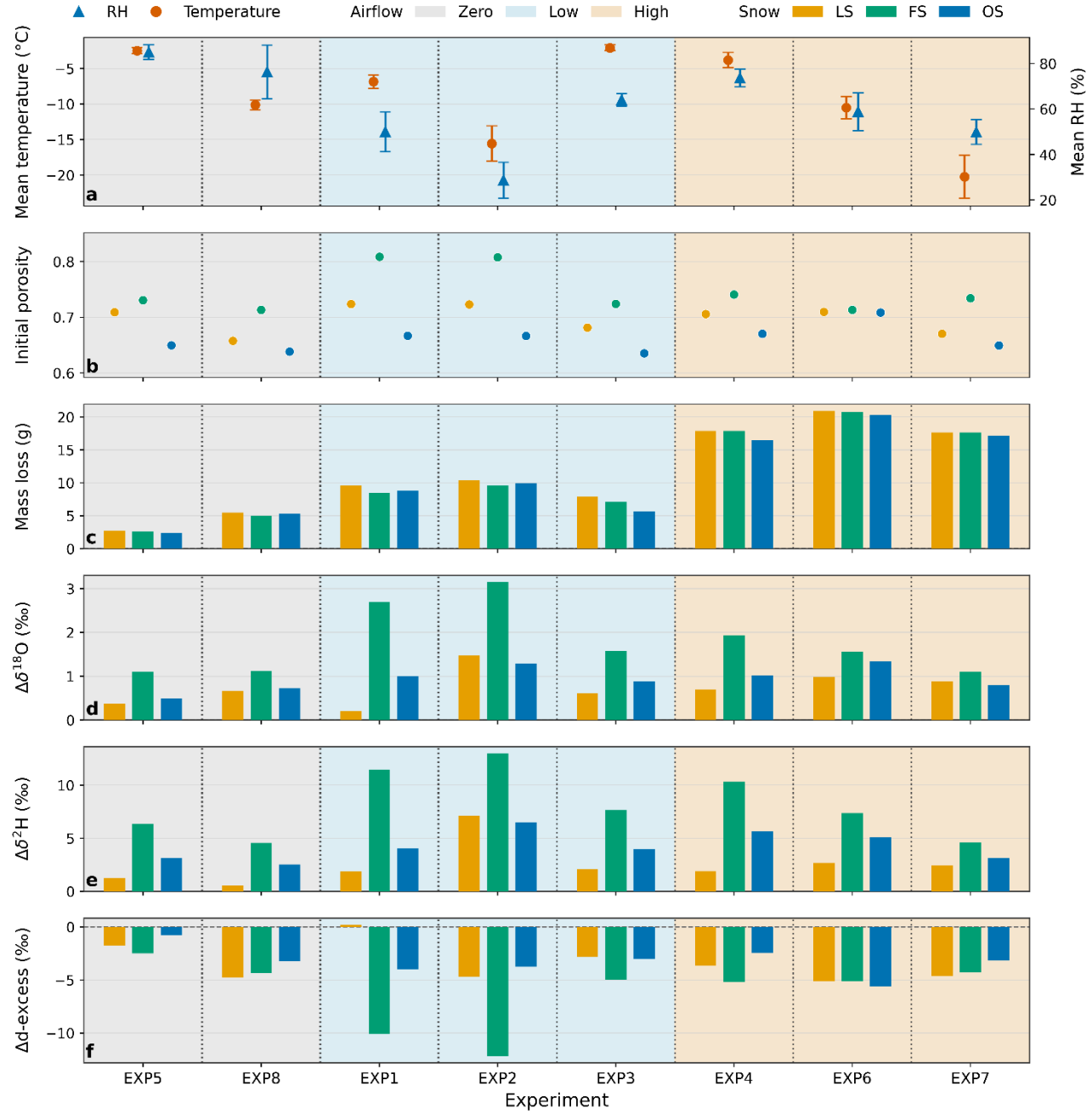

Figure 3. Sample properties, mass loss, and changes in isotopic composition across eight sublimation experiments grouped by airflow regime. (a) Mean tunnel air temperature (red circles, left axis) and mean relative humidity (blue triangles, right axis) during each experiment, with error bars showing standard deviation. (b) Initial bulk porosity for individual samples. (c) Total mass loss (g). (d–f) Changes in $\delta^{18}O$ (‰), $\delta^{2}H$ (‰), and d-excess (‰) between initial and final sampling stages. Background shading indicates airflow regime: peach = high airflow, blue = low airflow, grey = zero airflow. Vertical dotted lines separate individual experiments. Colours represent snow type: laboratory snow (LS, amber), fresh snow (FS, green), and old snow (OS, blue). Experiments are ordered along the x-axis by airflow regime.

https://doi.org/10.5194/egusphere-2026-2589
Preprint. Discussion started: 20 May 2026

3.2 Snow-type Isotopic Differences Persist after Mass Normalization

Sublimation magnitude differed substantially across airflow regimes, ranging from less than 3% to over 25% of initial sample mass. Direct comparison of absolute isotopic shifts therefore reflects both differences in isotopic response and differences in total sublimation. To compare isotopic change per unit mass loss, isotopic changes were normalized by sublimated mass (‰ g^{-1}) and by fractional mass loss (‰ per unit fractional mass loss). These metrics (Figure 4) allow comparison across experiments with differing sublimation magnitudes.

Mass-normalized isotopic changes were lowest under high airflow, while zero-airflow and low-airflow conditions produced larger but not strictly ordered responses. This pattern was clearest for $\delta^{18}O$ and $\delta^{2}H$ across all snow types. For example, mean $\delta^{18}O$ values in FS decreased from 0.323 ‰ g^{-1} under zero-airflow conditions to 0.289 ‰ g^{-1} under low airflow and 0.082 ‰ g^{-1} under high airflow. A similar decrease was observed for $\delta^{2}H$. For d-excess, mass-normalized values were negative across all airflow regimes and snow types but their dependence on airflow was less systematic than for $\delta^{18}O$ and $\delta^{2}H$.

Differences among snow types remained after normalization. For $\delta^{18}O$ and $\delta^{2}H$, FS exhibited the largest mass-normalized changes in all experiments, while LS showed the smallest values. OS generally showed intermediate values, although the ordering between OS and LS varied among experiments. For d-excess, FS exhibited the largest mass-normalized decreases in 5 of 8 experiments and in all low-airflow experiments. Under high-airflow and zero-airflow conditions, the ordering among snow types varied, with OS or LS occasionally showing the largest values.

These patterns are illustrated by comparison of experiments with similar thermal conditions but different airflow regimes (EXP5, EXP3, and EXP4). Under zero-airflow conditions in EXP5 (~85% RH), mass-normalized $\delta^{18}O$ and $\delta^{2}H$ values were high despite minimal mass loss. Under low airflow in EXP3 (~64% RH), intermediate values were observed. Under high airflow in EXP4 (~73% RH), mass-normalized values were lower despite larger mass losses. Across these experiments, FS exhibited the largest mass-normalized $\delta^{18}O$ and $\delta^{2}H$ values, while differences among snow types were smaller under high airflow.

Normalization by fractional mass loss produced similar patterns. FS showed the largest $\delta^{18}O$ and $\delta^{2}H$ values across all experiments, while OS and LS showed smaller values with variable ordering. For d-excess, variability among snow types was greater, and no consistent ordering was observed across experiments. Fraction-normalized values did not show reduced spread among snow types compared to mass-normalized values.

https://doi.org/10.5194/egusphere-2026-2589
Preprint. Discussion started: 20 May 2026

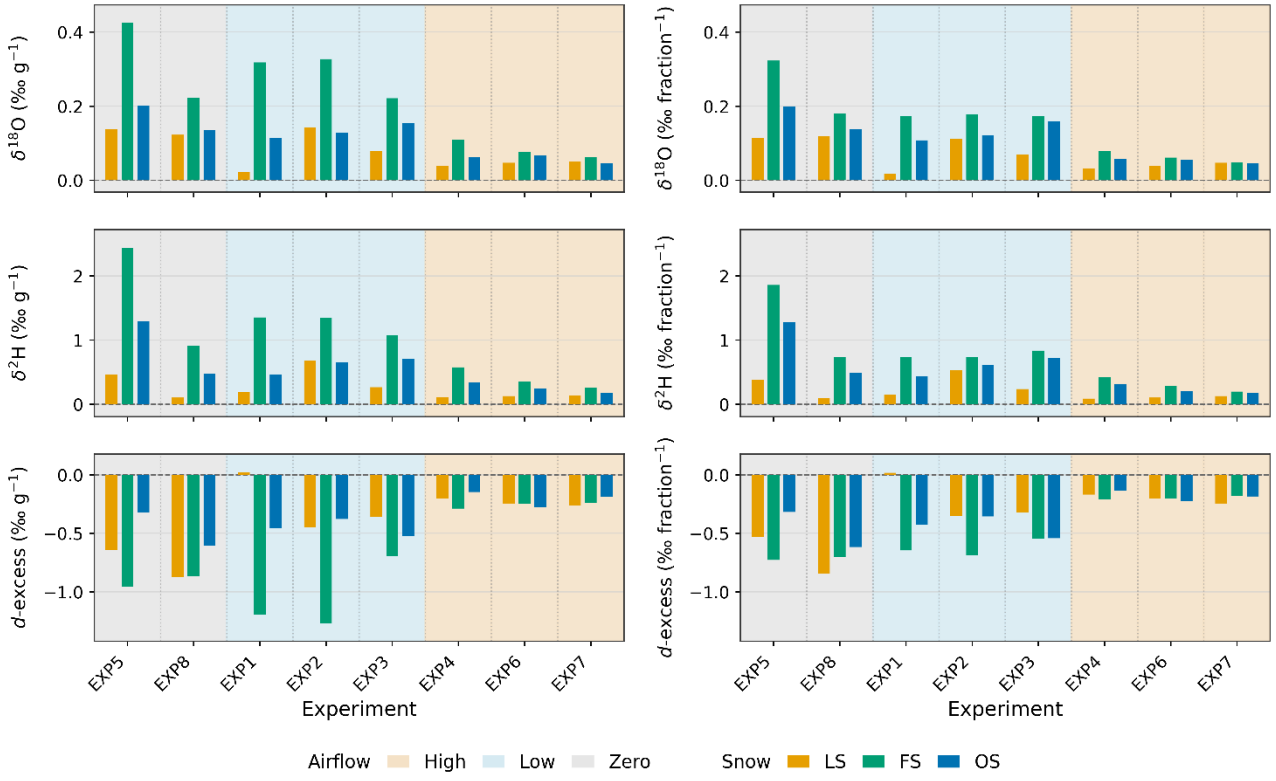

Figure 4. Mass-normalized (‰ g^{-1}) and fraction-normalized (‰ $fraction^{-1}$) isotopic change efficiency across eight sublimation experiments for $\delta^{18}O$, $\delta^{2}H$, and d-excess. IC and IC* represent the isotopic change per gram of mass lost and per unit fractional mass loss, respectively. Background shading indicates airflow regime: peach = high airflow, blue = low airflow, grey = zero airflow. Colours represent snow type: LS (amber), FS (green), OS (blue).

3.3 Initial Porosity as an Empirical Predictor of Isotopic Response in Natural Snow

To examine the role of snow structure, relationships between isotopic change and initial bulk porosity were evaluated across all experiments. In contrast to mass loss, which showed no systematic dependence on snow type within experiments (Section 3.1), isotopic changes showed systematic relationships with porosity, particularly for $\delta^{18}O$ and $\delta^{2}H$. Isotopic response was assessed using absolute isotopic change ($\Delta\delta$, ‰) and mass-normalized isotopic change (‰ g^{-1}).

Absolute isotopic change showed clear relationships with porosity in FS and when natural snow types were combined. For $\delta^{18}O$, isotopic change increased with porosity in FS ($r = 0.91$, $p = 0.002$) and OS ($r = 0.76$, $p = 0.028$). When FS and OS were combined, this relationship remained strong ($r = 0.90$, $p < 0.001$), and across all snow types $\delta^{18}O$ increased with porosity ($r = 0.75$, $p < 0.001$). For $\delta^{2}H$, isotopic change increased with porosity in FS ($r = 0.84$, $p = 0.010$), while OS showed a weaker and non-significant relationship ($p = 0.116$). When natural snow types were combined, $\delta^{2}H$ increased with porosity ($r = 0.87$, $p < 0.001$), and a significant relationship was also observed across all snow types ($r = 0.72$, $p < 0.001$).

https://doi.org/10.5194/egusphere-2026-2589
Preprint. Discussion started: 20 May 2026

For d-excess, isotopic change decreased with increasing porosity in FS ($r = -0.91$, $p = 0.002$), with more negative values at higher porosity. OS showed a weaker and non-significant relationship ($p = 0.078$), while the combined natural snow types showed a significant negative relationship ($r = -0.84$, $p < 0.001$). Across all snow types, d-excess decreased with increasing porosity ($r = -0.68$, $p < 0.001$).

Mass-normalized isotopic changes showed weaker and less consistent relationships with porosity. For $\delta^{18}O$, no significant relationship with porosity was observed within individual snow types, although significant positive relationships were observed when FS and OS were combined ($r = 0.54$, $p = 0.031$) and across all snow types ($r = 0.47$, $p = 0.021$). For $\delta^{2}H$, no statistically significant relationships with porosity were observed for any snow type or grouping (all $p \geq 0.051$). For d-excess, FS showed a negative but non-significant relationship with porosity ($r = -0.68$, $p = 0.062$), while OS and LS showed no significant relationships. When FS and OS were combined, a significant negative relationship was observed ($r = -0.65$, $p = 0.007$), and across all snow types ($r = -0.48$, $p = 0.019$).

https://doi.org/10.5194/egusphere-2026-2589
Preprint. Discussion started: 20 May 2026

Laboratory snow (LS) showed no significant relationships between porosity and isotopic change for any isotope metric ($\delta^{18}O$: r = 0.06, p = 0.883; $\delta^{2}H$: r = 0.50, p = 0.212; d-excess: r = 0.42, p = 0.294) (Figure 5), despite spanning a porosity range (0.66–0.72) that substantially overlaps the porosity range of OS (0.64–0.71), in which significant porosity–isotope relationships were observed. This suggests that the dependence of isotopic change on porosity is not controlled by bulk porosity magnitude alone. Although porosity ranges overlap among snow types, systematic differences in isotopic response persist, indicating that bulk porosity does not fully capture the relevant structural controls.

Temperature and RH were tested as alternative predictors of isotopic change (Figures S1 and S2). Temperature showed no significant relationships with isotopic change for any isotope metric or snow type (all $p \geq 0.086$; Figure S1). RH, in contrast, produced significant relationships in fresh snow consistent with kinetic-fractionation theory: lower RH was associated with more positive $\Delta\delta^{18}O$ ($r = -0.73$, $p = 0.039$) and more negative Δd-excess ($r = 0.84$, $p = 0.009$; Figure S2). Both signs match the expected response to stronger kinetic discrimination at lower humidity. Old snow showed no significant RH relationships, and laboratory snow showed only a single significant relationship ($\Delta\delta^{2}H$, $r = -0.84$, $p = 0.009$). None of the RH relationships were observed for mass-normalized isotopic change (all $p \geq 0.148$). The detection of the expected RH signal in fresh snow but not in old or laboratory snow suggests that snow structure modulates the expression of external fractionation forcing.

https://doi.org/10.5194/egusphere-2026-2589
Preprint. Discussion started: 20 May 2026

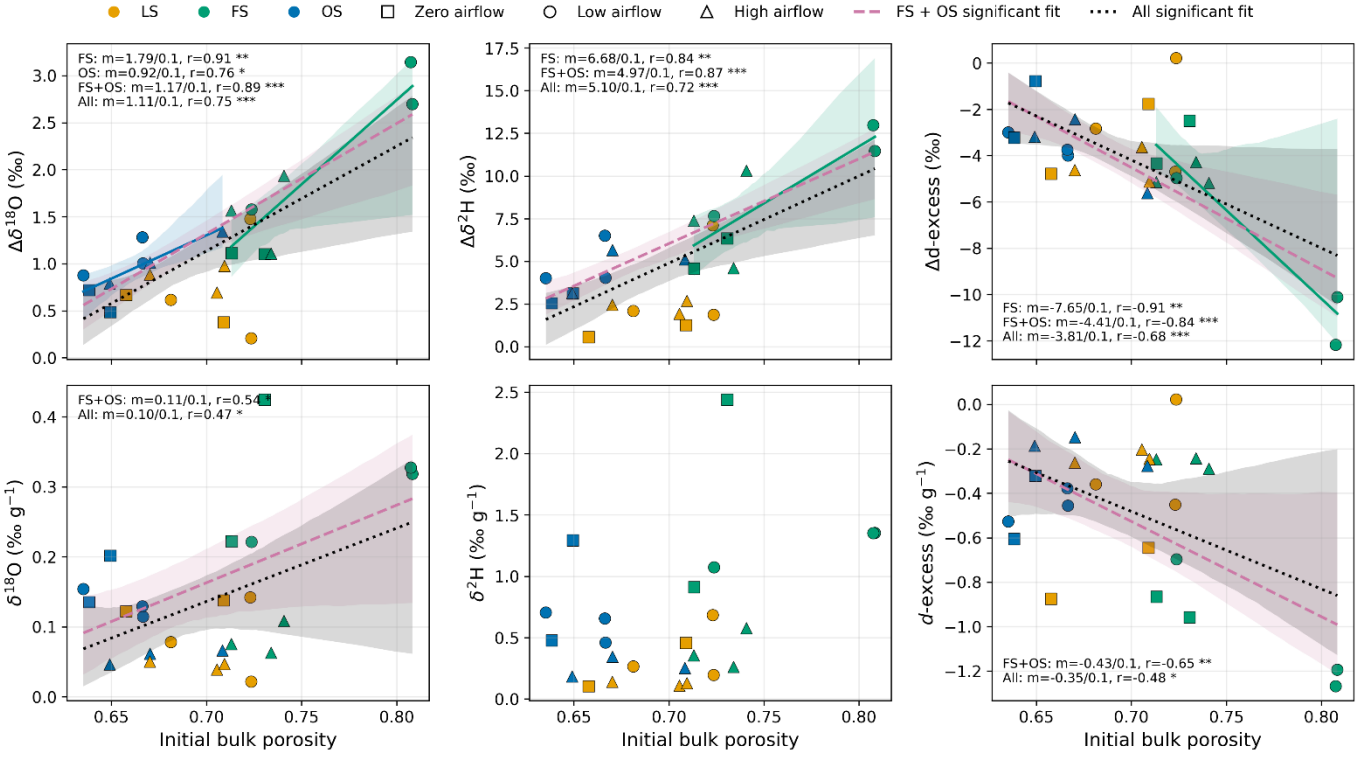

Figure 5. Relationship between initial bulk porosity and isotopic evolution under varying airflow conditions. The top row shows absolute isotopic change ($\Delta\delta^{18}O$, $\Delta\delta^{2}H$, and Δd-excess), while the bottom row shows mass-normalized isotopic change (‰ g^{-1}). Points are coloured by snow type (LS, FS, OS) and shaped by airflow regime (zero, low, high). Dashed lines represent significant regressions for combined FS+OS data, and dotted lines represent significant regressions for all snow types combined ($p < 0.05$). Shaded regions indicate 95% confidence intervals. Regression slope (m), correlation coefficient (r), and significance levels are reported where relationships are statistically significant

3.4 Qualitative Assessment of Temperature-Gradient Vapor-Flux Contributions

The experimental design imposed non-isothermal conditions with air-to-base-plate temperature differences (ΔT) ranging from 1.1°C to 19.3°C across experiments. ΔT is used here as a qualitative index of the thermal driving force for internal vapor flux rather than a direct measure of the temperature gradient within the snow, given the partial insulation provided by the polypropylene Petri dish walls and the three-dimensional thermal field arising from lateral heat exchange.

To assess whether TGM-driven vapor flux contributed to sublimation mass loss independently of surface atmospheric forcing, the vapor pressure deficit (VPD) was decomposed into a) an atmospheric component (the difference between saturation vapor pressure at the snow surface and actual vapor pressure in the tunnel air), b) an internal component (the difference between saturation vapor pressure at the base plate (−1°C) and at the snow surface, representing the thermodynamic driving force for upward vapor flux through the snow matrix). Snow surface temperature was approximated by the mean tunnel air temperature, which introduces uncertainty in vapor pressure deficit estimates.

https://doi.org/10.5194/egusphere-2026-2589
Preprint. Discussion started: 20 May 2026

The internal VPD ranged from 0.49 hPa (EXP 3, ΔT = 1.1°C) to 4.62 hPa (EXP 7, ΔT = 19.3°C), while the atmospheric VPD ranged from 0.51 to 1.85 hPa with no systematic relationship to ΔT (Figure S3A). These values carry uncertainty arising from the use of mean tunnel air temperature as a proxy for snow surface temperature. Under zero and low airflow conditions the ordering of mass loss across experiments follows the internal VPD rather than the atmospheric VPD (Figure S3B). Under zero airflow, EXP8 produced nearly twice the mass loss of EXP5 despite a smaller atmospheric VPD, consistent with TGM-driven base-to-surface vapor flux augmenting surface sublimation. Under low airflow, mass loss increased from EXP3 to EXP1 to EXP2 in direct correspondence with their internal VPDs (0.49, 2.20, and 4.06 hPa, respectively), despite EXP3 having the largest atmospheric VPD of the three. Under high airflow this pattern disappears, consistent with forced airflow dominating sublimation. These patterns suggest that TGM-driven vapor flux contributed to mass loss under low and zero airflow conditions.

Despite this contribution to mass loss, isotopic response was not enhanced in experiments with larger vapor pressure deficits. Across atmospheric, internal, and total VPD, neither absolute nor mass-normalized isotopic change increased systematically with VPD magnitude (Figures S4-S6). Holding airflow constant, larger temperature differences and larger internal VPDs did not produce greater absolute or mass-normalized isotopic change. This is opposite to what would be expected if TGM amplified bulk isotopic modification in proportion to thermal forcing. Because isotopic measurements were made on bulk-melted samples, any vertical isotopic gradients produced by temperature-gradient metamorphism would have been integrated into a single bulk value and cannot be evaluated directly.

3.5 Craig-Gordon Predictions Diverge from Observations Across Snow Types and Airflow Regimes

To test whether established kinetic-fractionation theory captures the snow-type differences observed, predicted isotopic changes from the Craig–Gordon (CG) framework were compared with measurements across all experiments. To eliminate the need for assumptions about ambient vapor isotopic composition, isotopic change was expressed in relative form ($\Delta\delta_{rel}$), the difference in isotopic change between two snow types within the same experiment. This framework cancels the shared atmospheric forcing and isolates snow-type-specific responses. Laboratory snow (LS) is used as the primary reference in the main text because it represents the structural end-member lacking natural formation history; analyses using FS and OS as reference are presented in Figures S7 and yield consistent results. Two CG formulations were evaluated: the conventional static formulation and a time-stepping formulation that updates the residual composition incrementally; both are described in Section 2.5.

Observed FS–LS relative isotopic changes were positive for $\delta^{18}O$ (range −0.20 to +2.49‰) and $\delta^{2}H$ (−0.61 to +9.60‰) across all airflow regimes, while FS d-excess decreased systematically relative to LS (range −10.32 to +1.56‰). The FS–LS contrast peaked under low airflow ($\delta^{18}O$: +1.71‰; $\delta^{2}H$: +7.01‰) and was smaller under high airflow ($\delta^{18}O$: +0.68‰; $\delta^{2}H$:

https://doi.org/10.5194/egusphere-2026-2589
Preprint. Discussion started: 20 May 2026

+5.08‰) and zero airflow ($\delta^{18}O$: +0.59‰; $\delta^{2}H$: +4.55‰). OS–LS contrasts were small for all isotope species and showed no consistent directional pattern across airflow regimes, in contrast to the systematic FS–LS depletion in d-excess.

The static CG formulation substantially overpredicted FS–LS relative isotopic change for $\delta^{18}O$ and $\delta^{2}H$ across all airflow regimes, with deviations largest under high airflow where predicted FS $\delta^{18}O$ reached +8.20‰ and $\delta^{2}H$ reached +65.6‰ against observed values of +0.68‰ and +5.08‰ (Figure 6, hollow symbols). Time-stepping reduced overprediction in every airflow regime, with the magnitude of improvement scaling with airflow intensity (Figure 6, filled symbols), but did not eliminate it. Time-stepping residuals were −1.49, −0.72, and −4.28‰ for $\delta^{18}O$ and −11.6, −11.9, and −34.6‰ for $\delta^{2}H$ under zero airflow, low airflow, and high airflow, respectively (Figure S8). Across all experiments, time-stepping CG predicted $\delta^{18}O$ spanning −1.14 to +7.04‰ and $\delta^{2}H$ spanning −8.05 to +55.3‰, against observed ranges of −0.20 to +2.49‰ and −0.61 to +9.60‰.

For d-excess, both CG formulations diverged in a qualitatively different way. Static CG predicted FS–LS d-excess changes spanning −1.32 to +1.09‰ across experiments, while observed values spanned −10.32 to +1.56‰ (Figure 6). Unlike for $\delta^{18}O$ and $\delta^{2}H$, the time-stepping formulation offered no improvement over static CG for d-excess in any airflow regime or snow-type pair. This asymmetry is diagnostic of the model limitation: reservoir updating reduces part of the $\delta^{18}O$ and $\delta^{2}H$ mismatch but does not improve d-excess predictions. Thus, the d-excess discrepancy reflects the inability of a single-stage surface-exchange formulation to represent the effective kinetic fractionation produced during vapor transport through porous snow.

The pattern of CG–observation divergence was consistent with the porosity ordering of the snow-type pairs. The largest and most systematic overprediction occurred for the FS–LS pair, which represents the largest porosity contrast in the dataset, and this overprediction grew with airflow intensity. OS–LS residuals were small and inconsistent in sign across airflow regimes ($\delta^{18}O$: −0.18, +1.06, −1.08‰; $\delta^{2}H$: −0.11, +6.97, −7.05‰ under zero airflow, low, and high airflow), consistent with the small porosity difference between LS and OS. Repeating the analysis with FS and OS as reference confirmed this scaling. Under OS reference, FS time-stepping residuals were −1.32, −1.78, and −3.20‰ for $\delta^{18}O$ and −11.5, −18.9, and −27.6‰ for $\delta^{2}H$ across airflow regimes. Under FS reference, OS residuals were the mirror image: +1.32, +1.78, and +3.20‰ for $\delta^{18}O$ and +11.5, +18.9, and +27.6‰ for $\delta^{2}H$. Within the relative comparison framework, CG systematically overestimates the isotopic change of the more porous snow type relative to the less porous reference, regardless of which serves as reference. For d-excess, range underprediction was consistent across all reference choices.

A sensitivity analysis was performed on the time-stepping CG formulation to determine whether snow-type differences in initial isotopic composition (δ^{0}) or fractional mass loss (f) could account for the predicted divergence (Section 2.5; Figures S9-S11). For the FS–LS pair, where δ^{0} differs by ~10‰, initial composition accounted for 49–82% of the predicted $\delta^{18}O$ relative change and f accounted for 14–44%. For the FS–OS pair, where δ^{0} differs by only ~1.5‰, f dominated (75–97%) while δ^{0} contributed 3–25%. The interaction term between δ^{0} and f was small across all pairs and airflow regimes, indicating

https://doi.org/10.5194/egusphere-2026-2589
Preprint. Discussion started: 20 May 2026

the two inputs act independently. Despite these differing relative weights, CG overestimated the isotopic change of FS relative to the less porous reference in both frameworks, and this overestimation grew with airflow intensity in both. For d-excess, the contributions of both δ^0 and f to predicted change were near zero, while the observed d-excess contrast reached −6.65‰ under low airflow. The model–observation divergence therefore cannot be attributed to differences in δ^0 or f between snow types for any isotope species.

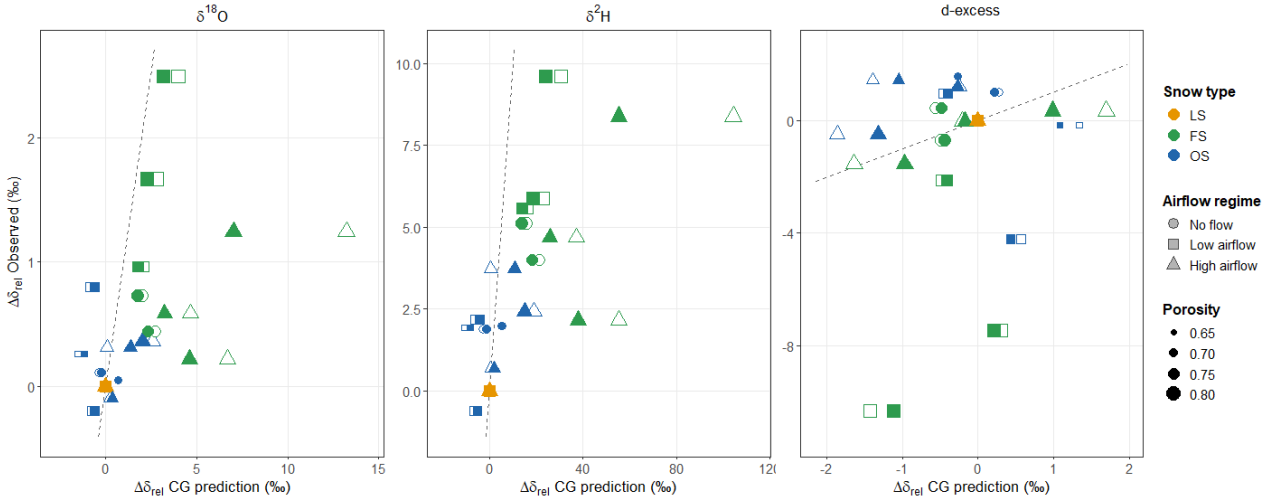

Figure 6. Observed versus Craig-Gordon (CG) predicted relative isotopic enrichment for (a) $\delta^{18}O$, (b) δ^2H, and (c) d-excess, referenced against laboratory snow (LS) within each experiment. The x-axis shows the CG-predicted relative change, and the y-axis shows the measured relative change. Symbol colour indicates snow type (LS: amber; FS: green; OS: blue), shape indicates airflow regime (circle: zero airflow; square: low airflow; triangle: high airflow), and size scales with initial bulk porosity. Hollow symbols represent the static CG formulation; filled symbols represent the time-stepping (finite-reservoir) CG formulation. The dashed line denotes the 1:1 relationship.

4. Discussion

4.1 Decoupling of Sublimation Rate and Isotopic Change

Across the imposed experimental conditions, airflow exerted the clearest control on sublimation mass loss. Boundary layer theory predicts that increasing airflow enhances sublimation by thinning the near-surface vapor gradient and increasing mass transfer efficiency. Sublimated mass scales with airflow across all experiments (Figure 3c), consistent with sublimation occurring under transport-limited conditions with reduced sensitivity to snow structure. This agrees with prior laboratory studies showing that sublimation rates scale with Reynolds number when vapor diffusion, rather than surface kinetics, limits mass transfer (Neumann et al., 2008).

https://doi.org/10.5194/egusphere-2026-2589
Preprint. Discussion started: 20 May 2026

In contrast, absolute isotopic changes (Δδ) show no consistent or monotonic dependence on airflow at the bulk sample scale (Figures 3d-f). This indicates that the total isotopic modification of the snowpack is not directly controlled by the amount of sublimation. Experiments with the largest mass losses do not necessarily produce the largest isotopic changes.

A clearer and more systematic pattern emerges when isotopic change is expressed per unit mass loss. Mass-normalized isotopic change was lowest under high airflow, particularly for $\delta^{18}O$ and $\delta^{2}H$, while zero-airflow and low-airflow conditions produced larger but not strictly monotonic responses (Figure 4). This indicates that strong airflow reduces isotopic change per unit mass loss.

This inverse relationship is consistent with a residence-time limitation on kinetic isotope fractionation. Because heavier isotopologues ($H_2{}^{18}O$ and H^2HO) diffuse more slowly through air than $H_2{}^{16}O$, kinetic fractionation requires a quasi-stagnant diffusive layer to persist long enough for isotopologue separation to develop (Merlivat, 1978). At the snow surface, turbulent mixing continuously thins and renews the diffusive sublayer, limiting the residence time over which isotopologue discrimination can develop (Merlivat and Coantic, 1975).

In addition to the surface process, a second mechanism may operate within the upper snow layers in the form of ventilation. Increased airflow may enhance vapor exchange between the pore space and the overlying atmosphere, reducing the residence time of vapor within the snow. Under such conditions, vapor generated within the pore network may be removed more rapidly, limiting the extent of isotopic modification that can accumulate during transport. In contrast, under low- and zero-airflow conditions, weaker ventilation allows longer residence times within the pore space, which may promote greater cumulative isotopic change. This interpretation is consistent with studies showing that wind-induced ventilation introduces an advective component to vapor transport in snowpacks (Sokratov and Sato, 2000) with exchange rates influenced by surface roughness and atmospheric turbulence (Bartlett and Lehning, 2011; Clifton et al., 2008). Because near-surface velocity and pore-space airflow were not measured, this ventilation interpretation remains qualitative.

Although airflow influences isotopic change per unit mass loss, it does not fully account for the differences observed between snow types. Variability among snow types persists under comparable atmospheric conditions. FS shows the strongest response for $\delta^{18}O$ and $\delta^{2}H$, whereas d-excess exhibits more variable ordering among snow types. Snow type differences are largest under low- and zero-airflow conditions and are reduced and become less systematic under high-airflow conditions. This suggests that airflow alone cannot explain the observed variability in isotopic change. Instead, these patterns point to an additional control linked to the internal structure of the snowpack, which governs the magnitude of isotopic modification.

https://doi.org/10.5194/egusphere-2026-2589
Preprint. Discussion started: 20 May 2026

4.2 Snow Structural State Modulates the Magnitude of Isotopic Change

The variability in isotopic response observed across experiments, together with the relationship between isotopic change and initial bulk porosity in natural snow (Section 3.3, Figure 5), indicates that snow structural state modulates the magnitude of isotopic change during sublimation. Because pore connectivity, tortuosity, permeability, and specific surface area were not measured directly, this interpretation should be viewed as an inference from bulk porosity and snow-type contrasts rather than as direct identification of the controlling microstructural variable.

The empirical relationship between porosity and isotopic change for natural snow suggests that bulk porosity captures part of the structural variability associated with isotopic response (Figure 5, Section 3.3). Although porosity is not itself a unique mechanistic driver, it likely covaries with properties of the snowpack, including pore connectivity, pathway tortuosity, permeability, and internal ice surface area, that regulate vapor transport. Snow is a bicontinuous porous medium in which the ice matrix and pore space are coupled through continuous vapor exchange (Löwe et al., 2011; Pinzer et al., 2012). Vapor generated at internal grain surfaces must diffuse through this pore network before escaping to the atmosphere. Along this pathway, isotopic fractionation occurs at repeated ice–vapor exchange steps, and total isotopic change builds up as vapor interacts with the ice matrix during transport (Casado et al., 2021; Ebner et al., 2017). The magnitude of isotopic change therefore depends on the effective length and complexity of vapor transport pathways, for which bulk porosity serves as a useful but imperfect observable proxy in natural snow.

The contrast between absolute and mass-normalized isotopic change provides further insight into how structure acts. For $\delta^{18}O$ and $\delta^{2}H$, the relationship with porosity is clearest for absolute $\Delta\delta$ and becomes weaker or absent when normalized by mass loss (Figure 5). This suggests that snow structure primarily modulates the total isotopic change that develops during sublimation, rather than the isotopic change associated with each unit of mass removed. More porous natural snow may exhibit larger isotopic changes because vapor transport pathways allow greater cumulative ice–vapor exchange before vapor escapes.

In contrast, d-excess retains a detectable dependence on structure even when expressed as mass-normalized isotopic change, indicating that structure influences kinetic fractionation. Given the sensitivity of d-excess to kinetic fractionation, this suggests that snow structure modifies the local vapor transport environment in ways that affect fractionation processes directly, beyond simply increasing the opportunity for isotopic change to build up.

The relationship between relative humidity and isotopic change provides additional context. Lower RH is expected to enhance kinetic discrimination, producing more positive $\Delta\delta^{18}O$ and more negative Δd-excess in residual snow (Merlivat, 1978). This expected paired response was clearest in fresh snow, where RH correlated negatively with $\Delta\delta^{18}O$ and positively

https://doi.org/10.5194/egusphere-2026-2589
Preprint. Discussion started: 20 May 2026

with Δd-excess. Its detection in the most porous natural snow type is consistent with structural amplification of external fractionation forcing through pore-network vapor recycling.

Microstructural evolution during sublimation may also contribute to the observed response. In highly porous, dendritic snow, curvature-driven sintering preferentially removes fine structures and progressively coarsens the matrix (Kaempfer and Schneebeli, 2007; Pinzer et al., 2012), altering pore geometry and internal surface area over time and thereby modifying vapor transport pathways. This effect would be most pronounced under low-airflow conditions, where longer vapor residence times allow the evolving microstructure to sustain repeated vapor–matrix interactions; under high airflow, rapid vapor removal limits its influence. Although this mechanism is not directly resolved in the present experiments, it provides a plausible additional link between snow metamorphism and isotopic response.

Airflow modulates, but does not override, this structural control. The development of isotopic differences likely requires sufficient residence time for vapor within the snowpack. Under low-airflow conditions, the diffusive sublayer remains relatively stable, allowing vapor emerging from the pore space to retain its isotopic signature and enabling structural differences to be expressed. Under high airflow, surface and internal ventilation (Section 4.1) reduce vapor residence time, suppressing isotopic change per unit mass loss and reducing differences between snow types. As a result, the influence of snow structure is most evident under zero- and low-airflow conditions, where pore-network vapor transport is least disturbed.

Within this framework, differences in isotopic change between fresh and older natural snow types reflect differences in effective pore structure rather than atmospheric forcing alone. As porosity decreases, vapor pathways may become more restricted, potentially limiting isotopic modification. An important exception is laboratory snow (LS), which shows no significant relationship between porosity and isotopic change despite spanning a comparable porosity range. This indicates that bulk porosity alone does not fully capture the relevant microstructural characteristics controlling isotopic evolution.

4.3 Laboratory Snow Decouples Bulk Porosity from Isotopic Response

We do not have direct measurements of pore connectivity or tortuosity in these experiments; the mechanistic link between bulk porosity and isotopic response is therefore an inference supported by the statistical relationship and the LS anomaly, rather than a directly demonstrated causal chain. With that caveat in mind, the absence of a significant relationship between bulk porosity and isotopic change in laboratory snow (LS), despite its porosity range overlapping that of fresh (FS) and old snow (OS), is both a limitation of bulk porosity as a predictor and a useful mechanistic clue. It indicates that the porosity-isotope relationship observed for natural snow cannot be generalized to all snow types, and that bulk porosity alone is insufficient as a universal predictor of isotopic response during sublimation. The LS anomaly suggests that two materials

https://doi.org/10.5194/egusphere-2026-2589
Preprint. Discussion started: 20 May 2026

may share similar porosity yet differ fundamentally in pore architecture, which modulates vapor transport and isotopic modification (Bellagamba et al., 2024).

Laboratory-generated snow lacks the natural formation history that builds the pore architecture responsible for isotopic response in natural snow. In natural snowpacks, curvature-driven sintering progressively strengthens inter-grain bonds, coarsens the ice matrix, and develops connected vapor pathways (Colbeck, 1997; Kaempfer and Schneebeli, 2007). The production method used here, following Schleef et al. (2014), involves deposition of ice crystals on a nucleation net followed by mechanical release and collection as bulk snow. This process does not reproduce the aggregation, settling, and sintering history through which natural snow develops its characteristic pore network. As a result, even when bulk porosity is similar, LS pore networks may differ in connectivity, tortuosity, permeability, specific surface area, or surface roughness from those of natural snow.

These structural differences directly influence vapor transport pathways and the extent of ice–vapor exchange, which together determine how much isotopic modification develops as vapor traverses the pore space before reaching the surface. The weaker and less systematic isotopic responses observed in LS relative to FS and OS are therefore more consistent with differences in pore network architecture than with differences in bulk porosity alone.

4.4 Temperature-Gradient Vapor Flux May Contribute to Mass Redistribution Without a Detectable Bulk Isotopic Signal

Temperature-gradient metamorphism (TGM) provides a mechanism for internal vapor transport within snowpacks that is physically distinct from surface sublimation. The mass loss data indicate that TGM contributed to total sublimation under low- and zero-airflow conditions (Section 3.4), consistent with its established role in natural snowpacks (Sturm and Benson, 1997). However, neither absolute nor mass-normalized isotopic change increased systematically with VPD or thermal forcing (Figures S3–S6). This suggests that temperature-gradient-driven vapor flux contributed to mass redistribution but did not produce a proportional change in bulk isotopic composition.

An explanation consistent with this pattern is a re-equilibration mechanism. This mechanism remains hypothetical in the present study because pore-space vapor isotope composition and depth-resolved snow isotope profiles were not measured. As TGM-driven vapor migrates upward through the pore network, repeated vapor-ice interactions may progressively buffer the isotopic signal toward equilibrium with the surrounding ice matrix, attenuating any fractionation imprint from the source depth. This buffering may become more effective under stronger temperature gradients, where higher vapor flux and longer transport pathways increase the number of vapor-crystal interactions per unit upward flux (Johnsen et al., 2000; Pinzer et al.,

https://doi.org/10.5194/egusphere-2026-2589
Preprint. Discussion started: 20 May 2026

2012). As a result, TGM contributes to mass redistribution without producing a proportionate isotopic signal at the bulk scale.

An alternative, and not mutually exclusive, explanation is that isotopic effects associated with TGM occur as internal gradients that are not resolved by bulk sampling. Vertical isotopic stratification may develop within the snowpack but be averaged out during bulk melting, resulting in little apparent change in the integrated isotopic signal. Distinguishing between these mechanisms would require depth-resolved isotope measurements combined with co-located temperature profiles.

4.5 Craig–Gordon Model–Data Mismatch Points to Missing Structural Representation

The results indicate limitations of applying a single-stage Craig–Gordon surface-exchange formulation to porous snow. Relative $\delta^{18}O$ and $\delta^{2}H$ residuals scale with porosity contrast between snow types and are largest under high airflow, while the observed range of d-excess change is substantially underpredicted (Figures 6, S7 and S8). These patterns persist after accounting for differences in initial isotope composition and remaining mass fraction between snow types (Figures S9-S11). Because ambient vapor isotope composition, snow surface temperature, pore-space humidity, and near-surface aerodynamic resistance were not directly measured, parameter uncertainty remains important. However, the systematic dependence of residuals on snow-type contrast and airflow regime suggests that missing structural representation is also required to explain the mismatch.

The CG framework treats the snowpack as a single effective surface-exchange process (Craig and Gordon, 1965; Dar et al., 2020). It does not represent the pore network through which vapor must diffuse before reaching the surface, where repeated ice–vapor exchange events can modify the cumulative isotopic signal in ways that depend on snow structure (Ebner et al., 2017; Touzeau et al., 2018). The model–observation discrepancies scale with porosity contrast, being largest for the FS–LS pair and smallest for OS–LS, consistent with these unrepresented internal processes contributing more strongly in natural snow types. This pattern is robust to the choice of reference snow type (Figure S7) and is also evident in the residual structure of the time-stepping model (Figure S8). The discrepancies also grow with airflow intensity. Observed isotopic contrasts between snow types are largest under low- and zero-airflow conditions. Under high airflow, surface and internal ventilation suppress per-gram fractionation across all snow types (Section 4.1) and observed differences between FS and the less porous snow types (OS, LS) shrink. CG, however, predicts comparable contrasts across airflow regimes because it has no snow-structural inputs through which airflow could differentially affect different snow types. The model–observation gap therefore widens at high airflow because the observations are compressing while CG's predictions are not, a consequence of the absence of structural representation in CG rather than evidence for an amplified internal mechanism.

The d-excess underprediction represents a qualitatively distinct failure mode. Because d-excess is sensitive to the differential molecular diffusivities of $H_2{}^{18}O$ and H^2HO, it is a particularly sensitive indicator of kinetic fractionation processes. The fact

https://doi.org/10.5194/egusphere-2026-2589
Preprint. Discussion started: 20 May 2026

that time-stepping recovers some of the missing variance for $\delta^{18}O$ and $\delta^{2}H$ but none for d-excess indicates that the d-excess failure does not arise from inappropriate reservoir treatment but from the effective kinetic fractionation pathway in porous snow not being represented by the single-stage surface-exchange formulation. This is consistent with d-excess responding to the structure of the fractionation pathway rather than its magnitude alone, but the present bulk measurements cannot identify the specific process responsible.

These results support a conceptual model in which airflow controls sublimation mass flux, whereas snow structure modulates how strongly that flux modifies snow isotopic composition (Figure 7).

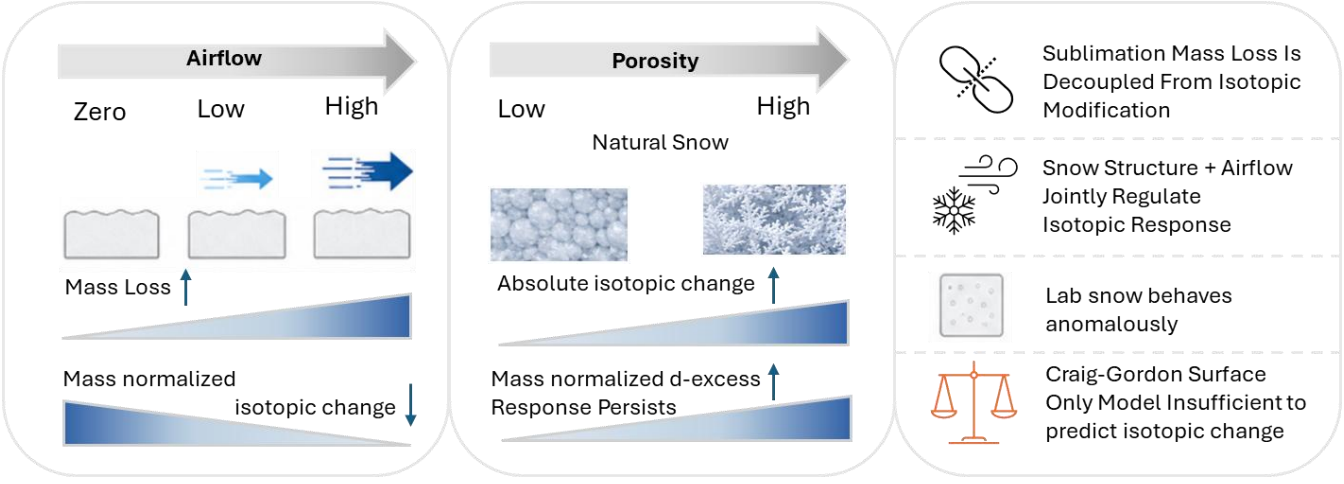

Figure 7. Conceptual summary of the controls on sublimation mass loss and isotopic modification in snow. Increasing airflow enhances sublimation mass loss but reduces mass-normalized isotopic change. In natural snow, increasing porosity is associated with larger isotopic change, while mass-normalized d-excess remains structure-dependent, indicating that pore-network structure also modifies the kinetic character of isotopic fractionation. Laboratory snow deviates from the natural-snow porosity relationship, showing that bulk porosity alone does not capture the structural controls on isotopic response. The Craig–Gordon framework treats sublimation as a surface-exchange process and therefore misses the snow-structure-dependent internal vapor transport processes. The schematic summarizes the decoupling between sublimation mass loss and isotopic modification and highlights why structure-independent fractionation models are incomplete for porous snow.

4.6 Experimental Limitations

Our wind-tunnel experiments were designed to bridge the gap between idealized laboratory studies and the physical complexity of natural snowpacks. By imposing a warm basal boundary (−1°C) against cold tunnel air, we created a vertical temperature gradient that promotes upward vapor transport and captures a key aspect of field-relevant thermal forcing absent from many prior isothermal sublimation experiments (e.g., Hughes et al., 2021; Sokratov and Golubev, 2009). The use of three structurally distinct snow types enabled isolation of structural effects from atmospheric forcing.

Several simplifications limit direct extrapolation to natural snowpacks. The experiments exclude processes that are common in the field, including melt-freeze cycles, liquid water percolation, radiative forcing, snowfall events, lateral moisture

https://doi.org/10.5194/egusphere-2026-2589
Preprint. Discussion started: 20 May 2026

transport, and interactions with impurities or biological material. Solar radiation can drive strong surface heating and sublimation under calm conditions, while nighttime radiative cooling may induce vapor deposition or surface hoar formation, producing diurnal cycles of isotopic modification that differ from the unidirectional forcing imposed here (Casado et al., 2021; Harris Stuart et al., 2023).

Additionally, the shallow sample depths (2 cm) limit the length of internal vapor pathways compared to natural snowpacks. Deeper snow would enhance internal vapor residence time and re-equilibration, potentially strengthening both structural control and buffering of temperature-gradient-driven transport. Because isotopic composition was measured on bulk-melted samples, any internal isotopic redistribution driven by temperature-gradient metamorphism would be averaged within each column rather than resolved vertically, meaning we cannot distinguish surface-driven change from deeper redistribution. Hence, the results should be interpreted as a process-level demonstration of coupled airflow and structural controls rather than a quantitative analogue of specific field settings.

The maximum tunnel airflow of ~3 m s^{-1} is modest, and the petri dish geometry introduces uncertainty: flow separation at the rim could reduce near-surface velocity, while rim-induced turbulence could enhance it. Shear-driven exchange between pore air and free atmosphere is generally limited to the upper few millimetres over flat snow surfaces (Clifton et al., 2008), though this varies with surface roughness and remains debated. The effective air penetration depth therefore cannot be determined from bulk tunnel measurements, limiting absolute interpretation of airflow effects. Nevertheless, the observed convergence of isotopic responses across snow types under high airflow is consistent with surface and internal ventilation (Section 4.1) suppressing per-gram fractionation across all snow types and compressing snow-type contrasts.

The snow surface temperature approximation used in the VPD decomposition (Section 3.4) introduces additional uncertainty. Because direct surface temperature measurements were unavailable, the mean tunnel air temperature was used as a proxy for snow surface temperature. This conflates surface and air temperatures and may over- or under-estimate the internal VPD component depending on the sign and magnitude of the actual surface-air temperature offset. The TGM analysis in Section 3.4 should therefore be interpreted as qualitative and directional rather than quantitative.

Future experiments could address these limitations by combining isotope measurements with direct observations of snow microstructure and vapor transport. Micro-CT imaging before and after sublimation would allow changes in pore connectivity, tortuosity, specific surface area, and grain morphology to be linked directly to isotopic change. Depth-resolved isotope sampling would help distinguish surface fractionation from internal redistribution, especially under imposed temperature gradients. Direct measurements of snow surface temperature, pore-space humidity, and pore-space vapor isotopic composition would allow the internal vapor pathway to be constrained rather than inferred. Wind-tunnel designs with deeper snow columns, flush-mounted samples, controlled surface roughness, and tracer-based airflow diagnostics could

https://doi.org/10.5194/egusphere-2026-2589
Preprint. Discussion started: 20 May 2026

further quantify the depth and strength of ventilation. Field experiments combining vertical isotope profiles, microstructure measurements, temperature gradients, radiation measurements, and wind profiles would provide the necessary link between the process-level controls identified here and the behavior of natural snowpacks.

4.7 Implications for Isotopic Archives, Snow Hydrology and Modelling

The structural dependence of sublimation-driven isotope change has implications for paleoclimate archives, hydrological applications, and snow isotope modelling. In each of these contexts, snow structure operates as an active control on isotopic evolution alongside atmospheric forcing. Because the experiments used shallow 2 cm samples under controlled wind-tunnel conditions, these implications should be interpreted as process-level guidance rather than direct quantitative scaling to natural snowpacks.

In the context of polar ice core and firn records, our results provide a mechanistic basis for post-depositional modification of the precipitation isotope signal prior to burial. Post-depositional vapor-snow exchange has been shown to modify surface snow isotopic composition between precipitation events at polar ice core sites (Steen-Larsen et al., 2013), with subsequent work demonstrating that sublimation fractionation specifically drives isotopic enrichment and d-excess depletion in ways that cannot be explained by equilibrium distillation alone (Casado et al., 2021; Hughes et al., 2021; Wahl et al., 2022). The structural dependence identified here implies that this overprint is not uniform: fresh, high-porosity snow shows a stronger isotopic response to sublimation than metamorphosed snow (Section 4.2), and this response is greatest under low-airflow conditions. At low-accumulation sites where surface snow remains exposed for extended periods before burial, two processes operate simultaneously. Ongoing sublimation continues to enrich the residual snow isotopically, while progressive metamorphism reduces its susceptibility to further fractionation. The result is a time-dependent, non-linear overprint that structure-independent correction schemes may misrepresent. The exceedingly low d-excess values in regions such as the McMurdo Dry Valleys and Allan Hills (Hu et al., 2022) are extreme expressions of this process. Structurally mediated sublimation fractionation operates across a continuum of environmental conditions and residence times, contributing to the warm-season bias in ice core isotope records (Wahl et al., 2022).

Beyond polar settings, mountain snowpacks can preserve a sublimation fingerprint in downstream archives. Munroe and Spötl (2026) document this in cave ice from the Uinta Mountains, Utah, which records a ~5000-year history of increasing sublimation efficacy through upward trends in $\delta^{18}O$ and $\delta^{2}H$ and declining d-excess, with the signal carried into the subsurface by infiltrating meltwater. This is consistent with the isotopic fingerprint produced in our experiments and supports that sublimation-driven fractionation constitutes a coherent, recordable signal across archive types and timescales well beyond the polar cryosphere.

https://doi.org/10.5194/egusphere-2026-2589
Preprint. Discussion started: 20 May 2026

From a hydrological perspective, sublimation alters the isotopic composition of residual snow and meltwater, with direct implications for tracer-based source partitioning. Snowmelt water is consistently found to be isotopically more enriched than mid-winter snowpack or accumulated precipitation samples, reflecting progressive sublimation-driven fractionation through the snow season (Beria et al., 2018; Ditlevsen et al., 2025; Noor et al., 2023b). Lechler and Niemi (2012) demonstrated that sublimation-induced isotopic shifts in high-elevation waters can affect stable isotope paleoaltimetry and catchment water balance estimates. Noor et al. (2023a) showed that using snowpack rather than actual meltwater as an isotopic endmember in hydrograph separation introduces systematic bias in meltwater contribution estimates. The structural dependence identified here complicates this interpretation: stratified snowpacks contain layers with differing structural properties, and therefore differing isotopic responses (Section 4.2), which means vertical isotopic heterogeneity within the snowpack cannot be predicted from sublimation mass alone. Current isotope-aided snow hydrology models largely do not account for sublimation-induced fractionation, or at best apply simplistic empirical approaches using a single calibrated fractionation parameter for the entire snowpack (Ala-aho et al., 2017; Schmieder et al., 2016). Our results suggest that incorporating snow structural state into isotope-based hydrological models could reduce systematic biases in meltwater composition predictions and improve water resource assessments in snow-dominated basins.

For snow isotope modelling, these findings motivate the development of porous-medium-based sublimation schemes in which isotopic fractionation depends on evolving microstructural properties rather than being prescribed as a constant parameter. Bulk porosity alone is insufficient to capture this behaviour, as suggested by the divergence between laboratory and natural snow at comparable porosities (Section 4.3). Microstructural descriptors such as specific surface area (SSA), pore connectivity, and tortuosity are more direct predictors of vapor-transport behaviour. These properties evolve predictably along the snow metamorphic trajectory and are already represented in advanced snow physics models such as CROCUSiso (Touzeau et al., 2018). Linking isotopic response to evolving SSA, which decays systematically with time and environmental forcing (Harris Stuart et al., 2023; Pinzer and Schneebeli, 2009) offers a tractable pathway toward incorporating structural control into isotope-enabled snow models without fundamentally redesigning existing frameworks. Achieving this will require coordinated laboratory measurements, field validation, and integration with snow microstructure evolution schemes.

5. Conclusions

Controlled wind-tunnel experiments across three snow types and three airflow regimes reveal a partial decoupling between sublimation mass loss and bulk isotopic change. Airflow produced the clearest control on sublimation mass loss, with high-airflow experiments generating the largest mass losses. However, these same high-airflow conditions produced the smallest isotopic changes per gram of sublimated snow. This indicates that conditions enhancing mass transfer do not necessarily enhance isotopic modification. The reduced mass-normalized isotope response under high airflow is consistent with

https://doi.org/10.5194/egusphere-2026-2589
Preprint. Discussion started: 20 May 2026

enhanced turbulent exchange and/or pore-space ventilation limiting the residence time over which kinetic fractionation can develop.

Snow structural state modulated the magnitude of sublimation-driven isotopic change. In natural snow types, bulk porosity was strongly associated with absolute changes in $\delta^{18}O$, $\delta^{2}H$, and d-excess, suggesting that microstructural properties linked to porosity influence the cumulative isotopic imprint of sublimation. For $\delta^{18}O$ and $\delta^{2}H$, the porosity relationship weakened after normalization by mass loss, suggesting that structure primarily affected the cumulative isotopic change that developed during sublimation. For d-excess, the porosity relationship persisted after mass normalization, suggesting that structural state also influenced the effective kinetic expression of fractionation per unit mass lost. Because pore connectivity, tortuosity, permeability, specific surface area, and surface roughness were not measured directly, bulk porosity should be interpreted as an empirical proxy for structural state rather than as the sole controlling variable.

Laboratory snow did not follow the natural-snow porosity–isotope relationship, despite overlapping the porosity range of old natural snow. This demonstrates that matching bulk porosity alone is insufficient to reproduce the isotopic behavior of natural snow. Snow formation history likely affects pore architecture, grain bonding, surface roughness, and vapor transport pathways, all of which may influence sublimation-driven isotope change. The weaker and less systematic isotope response of laboratory snow therefore highlights the need to distinguish between bulk structural metrics and the effective pore-network properties that govern vapor exchange.

The qualitative temperature-gradient analysis suggests that internal vapor flux may have contributed to mass redistribution under zero- and low-airflow conditions, but no systematic enhancement of bulk isotopic change was detected with increasing thermal forcing or vapor pressure deficit. Because isotope measurements were made on bulk-melted samples, any vertical isotopic gradients produced by temperature-gradient metamorphism would have been integrated into a single bulk value. Depth-resolved isotope measurements and direct snow-temperature profiles are therefore needed to separate surface sublimation effects from internal vapor redistribution.

Craig–Gordon surface-exchange predictions did not reproduce the observed snow-type contrasts. The model generally overestimated relative heavy-isotope enrichment and underrepresented the observed range of d-excess change, especially for the fresh snow–laboratory snow comparison. Time-stepping finite-reservoir calculations reduced part of the $\delta^{18}O$ and $\delta^{2}H$ mismatch but did not resolve the d-excess discrepancy. These results indicate that single-stage surface-fractionation formulations are incomplete for porous snow unless structural controls on internal vapor transport and effective kinetic fractionation are represented.

https://doi.org/10.5194/egusphere-2026-2589
Preprint. Discussion started: 20 May 2026

Overall, the isotopic imprint of sublimation depends not only on how much mass is lost, but also on snow structural state and airflow regime. Fresh, porous natural snow under low- or zero-airflow conditions can undergo stronger isotopic modification per unit mass loss than more compact or laboratory-produced snow, while high airflow can suppress snow-type differences by reducing the isotopic effect per unit sublimated mass. Models, correction schemes, and hydrological endmember approaches that neglect these controls may misrepresent sublimation-driven isotope signals in snow archives, meltwater, and snow-dominated catchments where snow structure and atmospheric exposure vary independently of sublimation flux.

Code and data availability

The data presented in this paper are provided in the Supplement Table S1 and will be uploaded to a public repository upon publication.

Author contributions

SSD and OS conceived and designed the experiments. SSD, OS, and VH conducted the experiments. SSD performed the formal analysis, prepared the visualizations, and wrote the original draft of the manuscript. OS, PA, BW, JW and HM contributed to data interpretation and manuscript revision. JH provided technical support for the operation of the Cold Climate Container (C3).

Competing interests

None of the authors have any competing interests.

Acknowledgements

We thank Lena M. Tallaksen for her facilitation and support of this study in her role as LATICE coordinator. We also thank Maisha Ahmed and Petra Korhonen for their contributions to sample preparation and isotopic analyses. During the preparation of this manuscript, the authors used generative AI tools (ChatGPT and Claude) for language refinement and to assist with Python code development for statistical analysis and figure preparation.

https://doi.org/10.5194/egusphere-2026-2589
Preprint. Discussion started: 20 May 2026

Financial support

SSD acknowledges funding from the Marie Skłodowska-Curie Actions European Postdoctoral Fellowship (Award no. 101062626, iSUBLIME-HORIZON-MSCA-2021-PF-01) and Maa- ja vesitekniikan tuki ry, Finland (23-11723-35, Sublimation Loss). OS acknowledges funding from the Research Council of Norway (NFR 336621, SNOWSUB). PA was supported by the Research Council of Finland, SNOMLT project (Award no. 347348). The Cold Climate Container is part of the infrastructure of the Strategic Research Initiative "Land Atmosphere Interactions in Cold Environments" (LATICE) at the University of Oslo (project number: UiO/GEO103920).

References

Ala-aho, P., Tetzlaff, D., McNamara, J. P., Laudon, H., Kormos, P., and Soulsby, C.: Modeling the isotopic evolution of snowpack and snowmelt: Testing a spatially distributed parsimonious approach, Water Resour. Res., 53, 5813–5830, https://doi.org/10.1002/2017WR020650, 2017.

Albert, M. R.: Effects of snow and firm ventilation on sublimation rates, Ann. Glaciol., 35, 52–56, https://doi.org/10.3189/172756402781817194, 2002.

Allan, R. P., Arias, P. A., Berger, S., Canadell, J. G., Cassou, C., Chen, D., Cherchi, A., Connors, S. L., Coppola, E., and Cruz, F. A.: Intergovernmental panel on climate change (IPCC). Summary for policymakers, in: Climate change 2021: The physical science basis. Contribution of working group I to the sixth assessment report of the intergovernmental panel on climate change, Cambridge University Press, 3–32, 2023.

Bartlett, S. J. and Lehning, M.: A theoretical assessment of heat transfer by ventilation in homogeneous snowpacks, Water Resour. Res., 47, https://doi.org/10.1029/2010WR010008, 2011.

Bellagamba, A. W., Berkelhammer, M., Hamed, Y., Pearce, K., and Steen-Larsen, H. C.: Isotopic Fractionation during Sublimation of Low Porosity Ice, Chem. Geol., 670, https://doi.org/10.1016/j.chemgeo.2024.122445, 2024.

Beria, H., Larsen, J. R., Ceperley, N. C., Michelon, A., Vennemann, T., and Schaefli, B.: Understanding snow hydrological processes through the lens of stable water isotopes, Wiley Interdisciplinary Reviews: Water, https://doi.org/10.1002/wat2.1311, 2018.

Calonne, N., Geindreau, C., Flin, F., Morin, S., Lesaffre, B., Rolland Du Roscoat, S., and Charrier, P.: 3-D image-based numerical computations of snow permeability: Links to specific surface area, density, and microstructural anisotropy, Cryosphere, 6, 939–951, https://doi.org/10.5194/tc-6-939-2012, 2012.

https://doi.org/10.5194/egusphere-2026-2589
Preprint. Discussion started: 20 May 2026

Calonne, N., Geindreau, C., and Flin, F.: Macroscopic modeling for heat and water vapor transfer in dry snow by homogenization, Journal of Physical Chemistry B, 118, 13393–13403, https://doi.org/10.1021/jp5052535, 2014.

Casado, M., Münch, T., and Laepple, T.: Climatic information archived in ice cores: Impact of intermittency and diffusion on the recorded isotopic signal in Antarctica, Climate of the Past, 16, 1581–1598, https://doi.org/10.5194/cp-16-1581-2020, 2020.

Casado, M., Landais, A., Picard, G., Arnaud, L., Dreossi, G., Stenni, B., and Prié, F.: Water Isotopic Signature of Surface Snow Metamorphism in Antarctica, Geophys. Res. Lett., 48, https://doi.org/10.1029/2021GL093382, 2021.

Clifton, A., Manes, C., Rüedi, J. D., Guala, M., and Lehning, M.: On shear-driven ventilation of snow, Boundary. Layer. Meteorol., 126, 249–261, https://doi.org/10.1007/s10546-007-9235-0, 2008.

Colbeck, S. C.: Theory of metamorphism of dry snow., J. Geophys. Res., 88, 5475–5482, https://doi.org/10.1029/JC088iC09p05475, 1983.

Colbeck, S. C.: A Review of Sintering in Seasonal Snow, 1997.

Craig, H. and Gordon, L.: Deuterium and oxygen 18 variations in the ocean and the marine atmosphere, 9–130 pp., 1965.

Dansgaard, W.: Stable isotopes in precipitation, Tellus, 16, 436–468, https://doi.org/10.3402/tellusa.v16i4.8993, 1964.

Dick, O., Calonne, N., Laurent, B., and Hagenmuller, P.: Monitoring dry snow metamorphism using 4D tomography across 20 experimental conditions, Earth Syst. Sci. Data, 18, 2875–2889, https://doi.org/10.5194/essd-18-2875-2026, 2026.

Ditlevsen, C., Marttila, H., and Ala-aho, P.: Stable Water Isotope Signal of Snow Meltwater: Testing Three Different Measurement Setups in Boreal-Subarctic Conditions, Hydrol. Process., 39, https://doi.org/10.1002/hyp.70277, 2025.

Earman, S., Campbell, A. R., Phillips, F. M., and Newman, B. D.: Isotopic exchange between snow and atmospheric water vapor: Estimation of the snowmelt component of groundwater recharge in the southwestern United States, Journal of Geophysical Research Atmospheres, 111, https://doi.org/10.1029/2005JD006470, 2006.

Ebner, P. P., Schneebeli, M., and Steinfeld, A.: Metamorphism during temperature gradient with undersaturated advective airflow in a snow sample, Cryosphere, 10, 791–797, https://doi.org/10.5194/tc-10-791-2016, 2016.

Ebner, P. P., Steen-Larsen, H. C., Stenni, B., Schneebeli, M., and Steinfeld, A.: Experimental observation of transient δ 18 O interaction between snow and advective airflow under various temperature gradient conditions, Cryosphere, 11, 1733–1743, 2017.

Ellehoj, M. D., Steen-Larsen, H. C., Johnsen, S. J., and Madsen, M. B.: Ice-vapor equilibrium fractionation factor of hydrogen and oxygen isotopes: Experimental investigations and implications for stable water isotope studies, Rapid Communications in Mass Spectrometry, 27, 2149–2158, https://doi.org/10.1002/rcm.6668, 2013.

Fourteau, K., Domine, F., and Hagenmuller, P.: Impact of water vapor diffusion and latent heat on the effective thermal conductivity of snow, Cryosphere, 15, 2739–2755, https://doi.org/10.5194/tc-15-2739-2021, 2021.

Gascoin, S.: Snowmelt and snow sublimation in the indus basin, Water (Switzerland), 13, https://doi.org/10.3390/w13192621, 2021.

https://doi.org/10.5194/egusphere-2026-2589
Preprint. Discussion started: 20 May 2026

Gat, J. R.: Oxygen and hydrogen isotopes in the hydrologic cycle, Annu. Rev. Earth Planet. Sci., 24, 225–262, https://doi.org/10.1146/annurev.earth.24.1.225, 1996.

Gottlieb, A. R. and Mankin, J. S.: Evidence of human influence on Northern Hemisphere snow loss, 625, https://doi.org/10.1038/s41586-023-06794-y, 2024.

Harris Stuart, R., Faber, A. K., Wahl, S., Hörhold, M., Kipfstuhl, S., Vasskog, K., Behrens, M., Zuhr, A. M., and Steen-Larsen, H. C.: Exploring the role of snow metamorphism on the isotopic composition of the surface snow at EastGRIP, Cryosphere, 17, 1185–1204, https://doi.org/10.5194/tc-17-1185-2023, 2023.

Hu, J., Yan, Y., Yeung, L. Y., and Dee, S. G.: Sublimation Origin of Negative Deuterium Excess Observed in Snow and Ice Samples From McMurdo Dry Valleys and Allan Hills Blue Ice Areas, East Antarctica, Journal of Geophysical Research: Atmospheres, 127, https://doi.org/10.1029/2021JD035950, 2022.

Hughes, A. G., Wahl, S., Jones, T. R., Zuhr, A., Hörhold, M., White, J. W. C., and Steen-Larsen, H. C.: The role of sublimation as a driver of climate signals in the water isotope content of surface snow: Laboratory and field experimental results, Cryosphere, 15, 4949–4974, https://doi.org/10.5194/tc-15-4949-2021, 2021.

Jafari, M., Gouttevin, I., Couttet, M., Wever, N., Michel, A., Sharma, V., Rossmann, L., Maass, N., Nicolaus, M., and Lehning, M.: The Impact of Diffusive Water Vapor Transport on Snow Profiles in Deep and Shallow Snow Covers and on Sea Ice, Front. Earth Sci. (Lausanne)., 8, https://doi.org/10.3389/feart.2020.00249, 2020.

Jafari, M., Sharma, V., and Lehning, M.: Convection of water vapour in snowpacks, J. Fluid Mech., 934, A38, 2022.

Johnsen, S. 1, Clausen, H. B., Cuffey, K. M., Hoffrnann, G., Schwander, J., and Creyts, T.: Diffusion of stable isotopes in polar firn and ice: the isotope effect in firn diffusion, Physics of Ice Core Records, 121–140, 2000.

Kaempfer, T. U. and Schneebeli, M.: Observation of isothermal metamorphism of new snow and interpretation as a sintering process, Journal of Geophysical Research Atmospheres, 112, https://doi.org/10.1029/2007JD009047, 2007.

Klein, E. S., Nolan, M., McConnell, J., Sigl, M., Cherry, J., Young, J., and Welker, J. M.: McCall Glacier record of Arctic climate change: Interpreting a northern Alaska ice core with regional water isotopes, Quat. Sci. Rev., 131, 274–284, https://doi.org/10.1016/j.quascirev.2015.07.030, 2016.

Laudon, H., Seibert, J., Köhler, S., and Bishop, K.: Hydrological flow paths during snowmelt: Congruence between hydrometric measurements and oxygen 18 in meltwater, soil water, and runoff, Water Resour. Res., 40, https://doi.org/10.1029/2003WR002455, 2004.

Lechler, A. R. and Niemi, N. A.: The influence of snow sublimation on the isotopic composition of spring and surface waters in the southwestern United States: Implications for stable isotope-based paleoaltimetry and hydrologic studies, Bulletin of the Geological Society of America, https://doi.org/10.1130/B30467.1, 2012.

Löwe, H., Spiegel, J. K., and Schneebeli, M.: Interfacial and structural relaxations of snow under isothermal conditions, Journal of Glaciology, 57, 499–510, https://doi.org/10.3189/002214311796905569, 2011.

https://doi.org/10.5194/egusphere-2026-2589
Preprint. Discussion started: 20 May 2026

MacGregor, J. A., Fahnestock, M. A., Colgan, W. T., Larsen, N. K., Kjeldsen, K. K., and Welker, J. M.: The age of surface-exposed ice along the northern margin of the Greenland Ice Sheet, Journal of Glaciology, 66, 667–684, https://doi.org/10.1017/jog.2020.62, 2020.

Madsen, M. V., Steen-Larsen, H. C., Hörhold, M., Box, J., Berben, S. M. P., Capron, E., Faber, A. K., Hubbard, A., Jensen, M. F., Jones, T. R., Kipfstuhl, S., Koldtoft, I., Pillar, H. R., Vaughn, B. H., Vladimirova, D., and Dahl-Jensen, D.: Evidence of Isotopic Fractionation During Vapor Exchange Between the Atmosphere and the Snow Surface in Greenland, Journal of Geophysical Research: Atmospheres, 124, 2932–2945, https://doi.org/10.1029/2018JD029619, 2019.

Mankin, J. S., Viviroli, D., Singh, D., Hoekstra, A. Y., and Diffenbaugh, N. S.: The potential for snow to supply human water demand in the present and future, Environmental Research Letters, 10, https://doi.org/10.1088/1748-9326/10/11/114016, 2015.

Merlivat, L.: Molecular diffusivities of H216O, HD16O, and H218O in gases, J. Chem. Phys., 69, 2864–2871, https://doi.org/10.1063/1.436884, 1978.

Merlivat, L. and Coantic, M.: Study of mass transfer at the air-water interface by an isotopic method, J. Geophys. Res., 80, 3455–3464, https://doi.org/10.1029/jc080i024p03455, 1975.

Mote, P. W., Li, S., Lettenmaier, D. P., Xiao, M., and Engel, R.: Dramatic declines in snowpack in the western US, NPJ Clim. Atmos. Sci., 1, https://doi.org/10.1038/s41612-018-0012-1, 2018.

Munroe, J. and Spötl, C.: Stable isotopes in cave ice reveal Holocene changes in mountain snowpack sublimation, Geology, https://doi.org/10.1130/G54328.1, 2026.

Neumann, T. A. and Waddington, E. D.: Effects of firn ventilation on isotopic exchange, Journal of Glaciology, 50, 183–192, https://doi.org/10.3189/172756504781830150, 2004.

Neumann, T. A., Albert, M. R., Lomonaco, R., Engel, C., Courville, Z., and Perron, F.: Experimental determination of snow sublimation rate and stable-isotopic exchange, Ann. Glaciol., https://doi.org/10.3189/172756408787814825, 2008.

Noor, K., Marttila, H., Welker, J. M., Mustonen, K. R., Kløve, B., and Ala-aho, P.: Snow sampling strategy can bias estimation of meltwater fractions in isotope hydrograph separation, J. Hydrol. (Amst)., 627, https://doi.org/10.1016/j.jhydrol.2023.130429, 2023a.

Noor, K., Marttila, H., Klöve, B., Welker, J. M., and Ala-aho, P.: The Spatiotemporal Variability of Snowpack and Snowmelt Water 18O and 2H Isotopes in a Subarctic Catchment, Water Resour. Res., 59, https://doi.org/10.1029/2022WR033101, 2023b.

Pinzer, B. R. and Schneebeli, M.: Snow metamorphism under alternating temperature gradients: Morphology and recrystallization in surface snow, Geophys. Res. Lett., 36, https://doi.org/10.1029/2009GL039618, 2009.

Pinzer, B. R., Schneebeli, M., and Kaempfer, T. U.: Vapor flux and recrystallization during dry snow metamorphism under a steady temperature gradient as observed by time-lapse micro-tomography, Cryosphere, 6, 1141–1155, https://doi.org/10.5194/tc-6-1141-2012, 2012.

https://doi.org/10.5194/egusphere-2026-2589
Preprint. Discussion started: 20 May 2026

Reba, M. L., Pomeroy, J., Marks, D., and Link, T. E.: Estimating surface sublimation losses from snowpacks in a mountain catchment using eddy covariance and turbulent transfer calculations, Hydrol. Process., 26, 3699–3711, https://doi.org/10.1002/hyp.8372, 2012.

Schleef, S., Jaggi, M., Löwe, H., and Schneebeli, M.: Instruments and methods: An improved machine to produce nature-identical snow in the laboratory, Journal of Glaciology, 60, 94–102, https://doi.org/10.3189/2014JoG13J118, 2014.

Schmieder, J., Hanzer, F., Marke, T., Garvelmann, J., Warscher, M., Kunstmann, H., and Strasser, U.: The importance of snowmelt spatiotemporal variability for isotope-based hydrograph separation in a high-elevation catchment, Hydrol. Earth Syst. Sci., 20, 5015–5033, https://doi.org/10.5194/hess-20-5015-2016, 2016.

Schneebeli, M. and Sokratov, S. A.: Tomography of temperature gradient metamorphism of snow and associated changes in heat conductivity, Hydrol. Process., 18, 3655–3665, 2004.

Sexstone, G. A., Clow, D. W., Fassnacht, S. R., Liston, G. E., Hiemstra, C. A., Knowles, J. F., and Penn, C. A.: Snow Sublimation in Mountain Environments and Its Sensitivity to Forest Disturbance and Climate Warming, Water Resour. Res., 54, 1191–1211, https://doi.org/10.1002/2017WR021172, 2018.

Shabir Dar, S., Ghosh, P., Swaraj, A., and Kumar, A.: Craig-Gordon model validation using stable isotope ratios in water vapor over the Southern Ocean, Atmos. Chem. Phys., 20, 11435–11449, https://doi.org/10.5194/acp-20-11435-2020, 2020.

Sokratov, S. A. and Golubev, V. N.: Snow isotopic content change by sublimation, Journal of Glaciology, 55, 823–828, https://doi.org/10.3189/002214309790152456, 2009.

Sokratov, S. A. and Sato, A.: Wind propagation to snow observed in laboratory, Ann. Glaciol., 31, 427–431, https://doi.org/10.3189/172756400781820020, 2000.

Sprenger, M., Carroll, R. W. H., Dennedy-Frank, J., Siirila-Woodburn, E. R., Newcomer, M. E., Brown, W., Newman, A., Beutler, C., Bill, M., Hubbard, S. S., and Williams, K. H.: Variability of Snow and Rainfall Partitioning Into Evapotranspiration and Summer Runoff Across Nine Mountainous Catchments, Geophys. Res. Lett., 49, https://doi.org/10.1029/2022GL099324, 2022.

Steen-Larsen, H. C., Johnsen, S. J., Masson-Delmotte, V., Stenni, B., Risi, C., Sodemann, H., Balslev-Clausen, D., Blunier, T., Dahl-Jensen, D., Ellehøj, M. D., Falourd, S., Grindsted, A., Gkinis, V., Jouzel, J., Popp, T., Sheldon, S., Simonsen, S. B., Sjolte, J., Steffensen, J. P., Sperlich, P., Sveinbjörnsdóttir, A. E., Vinther, B. M., and White, J. W. C.: Continuous monitoring of summer surface water vapor isotopic composition above the Greenland Ice Sheet, Atmos. Chem. Phys., 13, 4815–4828, https://doi.org/10.5194/acp-13-4815-2013, 2013.

Stigter, E. E., Litt, M., Steiner, J. F., Bonekamp, P. N. J., Shea, J. M., Bierkens, M. F. P., and Immerzeel, W. W.: The Importance of Snow Sublimation on a Himalayan Glacier, Front. Earth Sci. (Lausanne)., 6, https://doi.org/10.3389/feart.2018.00108, 2018.

Strasser, U., Bernhardt, M., Weber, M., Liston, G. E., and Mauser, W.: The Cryosphere Is snow sublimation important in the alpine water balance?, The Cryosphere, 53–66 pp., 2008.

https://doi.org/10.5194/egusphere-2026-2589
Preprint. Discussion started: 20 May 2026

Sturm, M. and Benson, C. S.: Vapor transport, grain growth and depth-hoar development in the subarctic snow, Journal of Glaciology, 43, 42–58, https://doi.org/10.3189/s0022143000002793, 1997.

Touzeau, A., Landais, A., Morin, S., Arnaud, L., and Picard, G.: Numerical experiments on vapor diffusion in polar snow and firn and its impact on isotopes using the multi-layer energy balance model Crocus in SURFEX v8.0, Geosci. Model Dev., 11, 2393–2418, https://doi.org/10.5194/gmd-11-2393-2018, 2018.

Wahl, S., Steen-Larsen, H. C., Hughes, A. G., Dietrich, L. J., Zuhr, A., Behrens, M., Faber, A., and Hörhold, M.: Atmosphere-snow exchange explains surface snow isotope variability, Geophys. Res. Lett., 49, e2022GL099529, 2022.

Wahl, S., Walter, B., Aemisegger, F., Bianchi, L., and Lehning, M.: Identifying airborne snow metamorphism with stable water isotopes, Cryosphere, 18, 4493–4515, https://doi.org/10.5194/tc-18-4493-2024, 2024.